Feasibility of measuring the Λc baryon electromagnetic moments at LHC using crystals

Alex Fomin

contributed by:

S. Barsuk (IJCLab), O.A. Bezshyyko (KNU), L. Burmistrov (IJCLab), G. Calderini (LPNHE), S.P. Fomin (KIPT, KhNU), Yu. Ivanov (PNPI), I.V. Kirillin (KIPT, KhNU), A.Yu. Korchin (KIPT, KhNU), V.A. Kovalchuk (KIPT, KhNU), E. Kou (IJCLab), M. Liul (LAL, KhNU), L. Massacrier (IPN), D.Mirarchi (CERN), A. Natochii (LAL, KNU), E. Niel (IJCLab), S. Redaelli (CERN), P. Robbe (IJCLab), W. Scandale (CERN), N.F. Shul'ga (KIPT, KhNU), A. Stocchi (IJCLab)

université PARIS-SACLAY

cnrs

IJCLab Irène Joliot-Curie Laboratoire de Physique des 2 Infinis

Outline

Introduction

- Electromagnetic moments of baryons
- Spin precession in a bent crystal

Optimal crystal orientation for EDM measurement [1,2]

- Spin precession in a bent crystal
- Initial polarisation of baryons [1,2]
- quantitive analysis

MDM of Σ+ (experiment E761, Fermilab 1990) [3]

- Mirroring the setup
- Cancelation of apparatus biases

Performance assessment of layouts in IR3 and IR8 [4,5,1]

- Double crystal layouts at LHC [4,5]
- Precision of measurement [1]
- Possible improvements [1,4]

[1] A.S. Fomin et al. Eur. Phys. J. C (2020) 80:358

[2] A.S. Fomin, JHEP 08 (2017) 120

[3] D. Chen, PhD thesis, SUNY, Albany, 1992.

[4] D. Mirarchi et al. Eur. Phys. J. C 80 (2020) 10, 929

[5] CERN Yellow Reports: Monographs, 4/2020

Electromagnetic moments of baryons

Magnetic Dipole Moment:

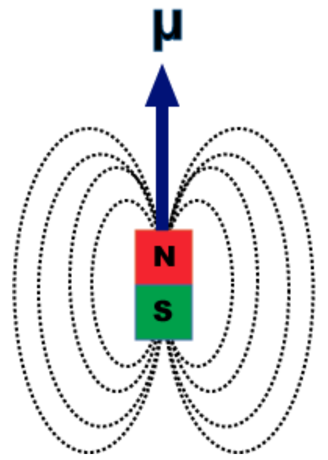

$$\vec{\mu} = \frac{g}{2}\frac{e}{m}\vec{S}, \quad \vec{S} = \frac{\hbar}{2}\vec{\sigma}$$

$|g| = 2$ → a point-like Dirac particle

$|g| \approx 2$ → a radiative corrections

$|g| \neq 2$ → a composite structure or NP

Particle	cτ	*g*-factor	Comments	
p	∞	+ 5.585 694 702 (17)	exp.	
n	~∞	– 3.826 085 45 (90)	exp.	
Σ^+	2.4 cm	+ 6.233 (25)	exp.	world-average value
		+ 6.1 $(12)_{stat}$ $(10)_{syst}$	exp.	using Bent Crystals (at Fermilab 1990)
Λ_c^+	60 μm	+ 1.90 (15)	theor.	assuming $g_c \approx 2$
		not measured	exp.	Feasibility studies at LHC

Electric Dipole Moment:

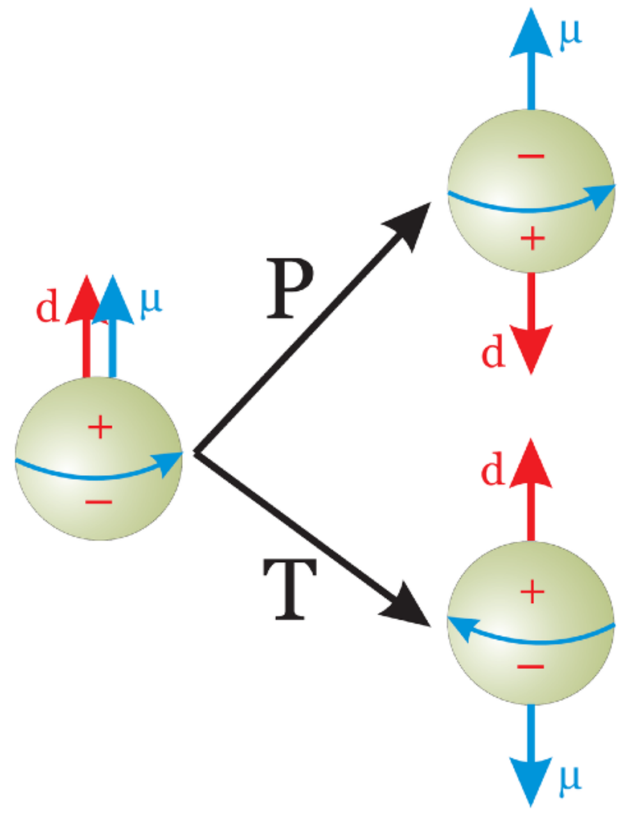

$$\vec{\delta} = \frac{f}{2}\frac{e}{m}\vec{S}, \quad \vec{S} = \frac{\hbar}{2}\vec{\sigma}$$

A nonzero value is forbidden by both:

T invariance and P invariance.

Particle	$\lvert\delta\rvert$, e cm 10^{-25}
p	< 2.1
n	< 0.18
Σ^+	not measured
Λ_c^+	not measured

Spin precession in a bent crystal

- V.G. Baryshevsky, Sov. Tech. Phys. Lett. 5 (1979) 73.
- V.L. Lyuboshits, Sov. J. Nucl. Phys. 31 (1980) 509 [inSPIRE].

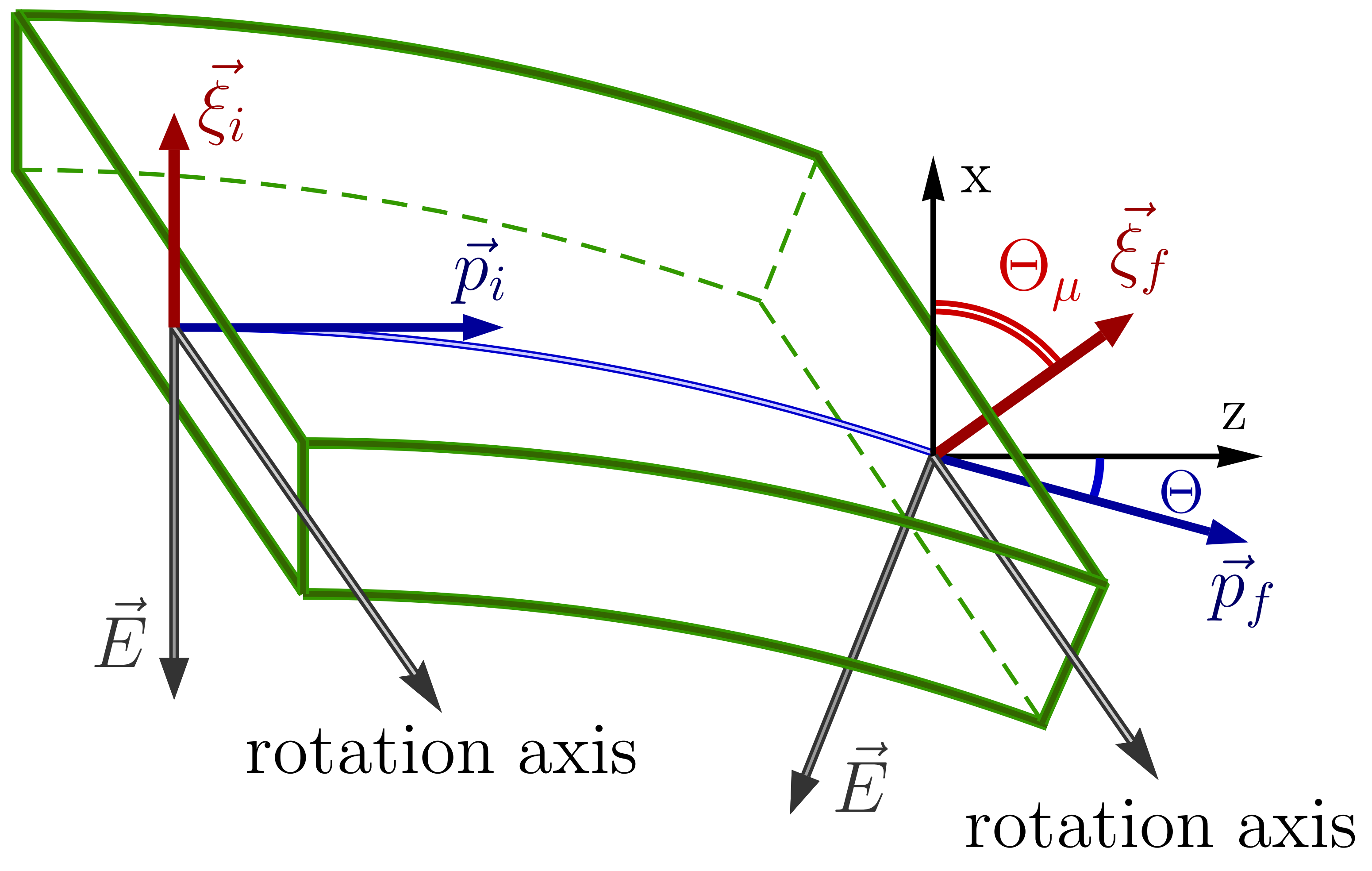

$$\boxed{\Theta_\mu \equiv \angle(\xi_i\,\xi_f) = (1+\gamma a)\,\Theta} \qquad a = \frac{g-2}{2}, \qquad \Theta = \frac{L}{R}$$

$\gamma,\ g,\ a$ – Lorentz factor, g-factor, anomalous MDM of Λ_c

$\Theta,\ L,\ R$ – deflecting angle, length, curvature radius of the crystal

Initial Polarisation:

$$\vec{\xi}_i = \xi\,(\ 1\ ,\ 0\ ,\ 0\ )$$

Final polarisation

$$\vec{\xi}_f = \xi\,(\cos\Theta_\mu,\ 0\ ,\ \sin\Theta_\mu)$$

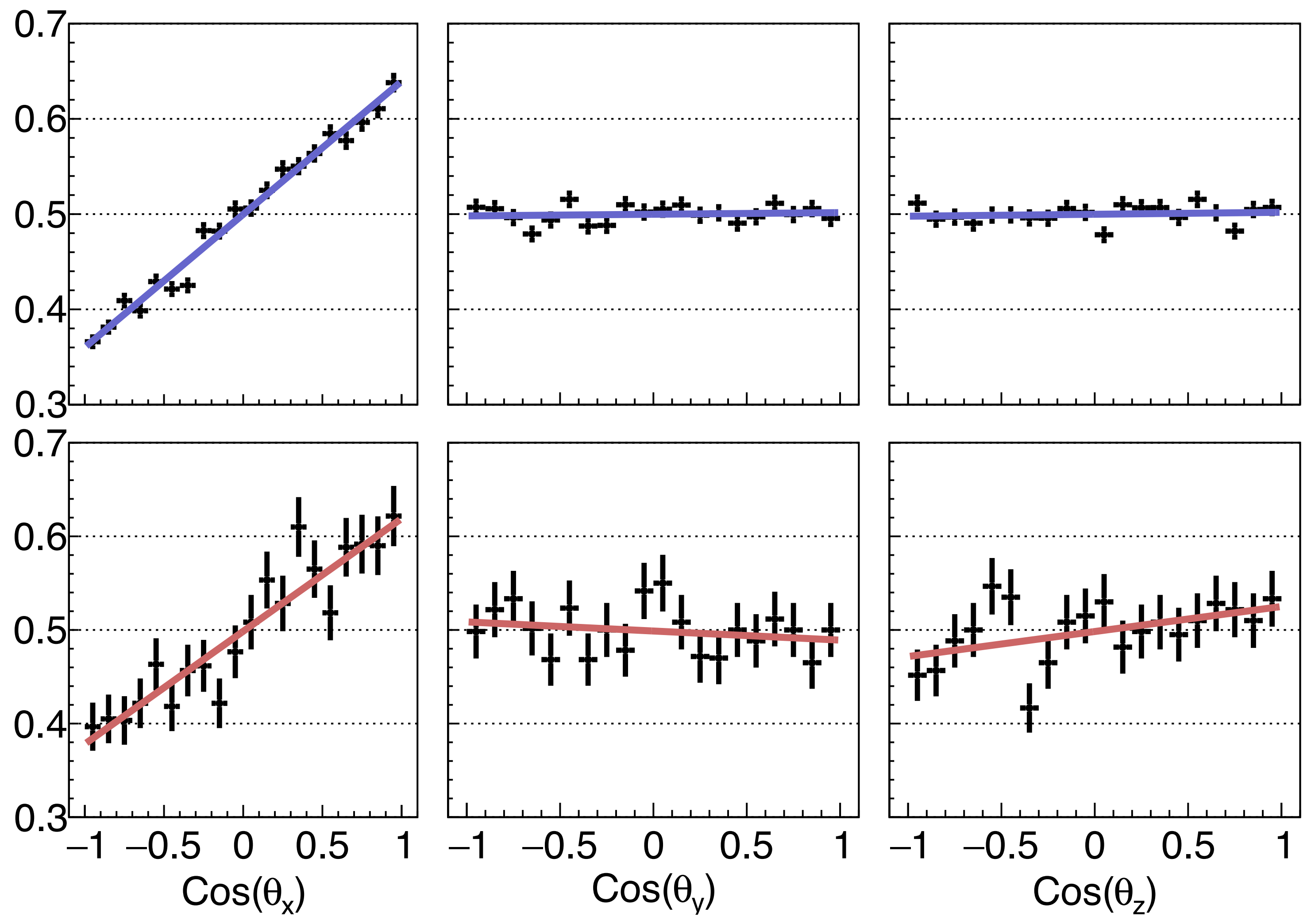

$$\Lambda_c^+ \to Meson + Baryon$$

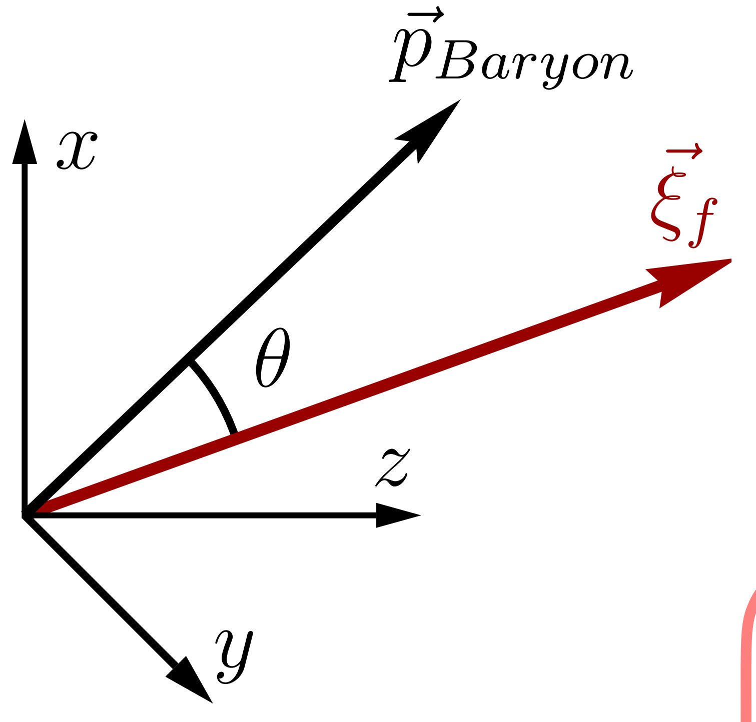

$$\frac{dN}{d\cos\theta_z} = \frac{1}{2}\left(1 + \alpha\,\xi_{fz}\cos\theta_z\right)$$

$$\boxed{b \equiv \alpha\,\xi\,\Theta_\mu \qquad \Delta b = \sqrt{\frac{3}{N}}}$$

$$\boxed{\Delta g = \frac{2}{\alpha\,\langle \xi\gamma\rangle\,\Theta}\sqrt{\frac{3}{N}}}$$

Optimal crystal orientation for EDM measurement

Optimal crystal orientation for MDM and EDM measurements

V.G. Baryshevsky,
Sov. Tech. Phys. Lett. 5 (1979) 73.

V.L. Lyuboshits,
Sov. J. Nucl. Phys. 31 (1980) 509 [inSPIRE].

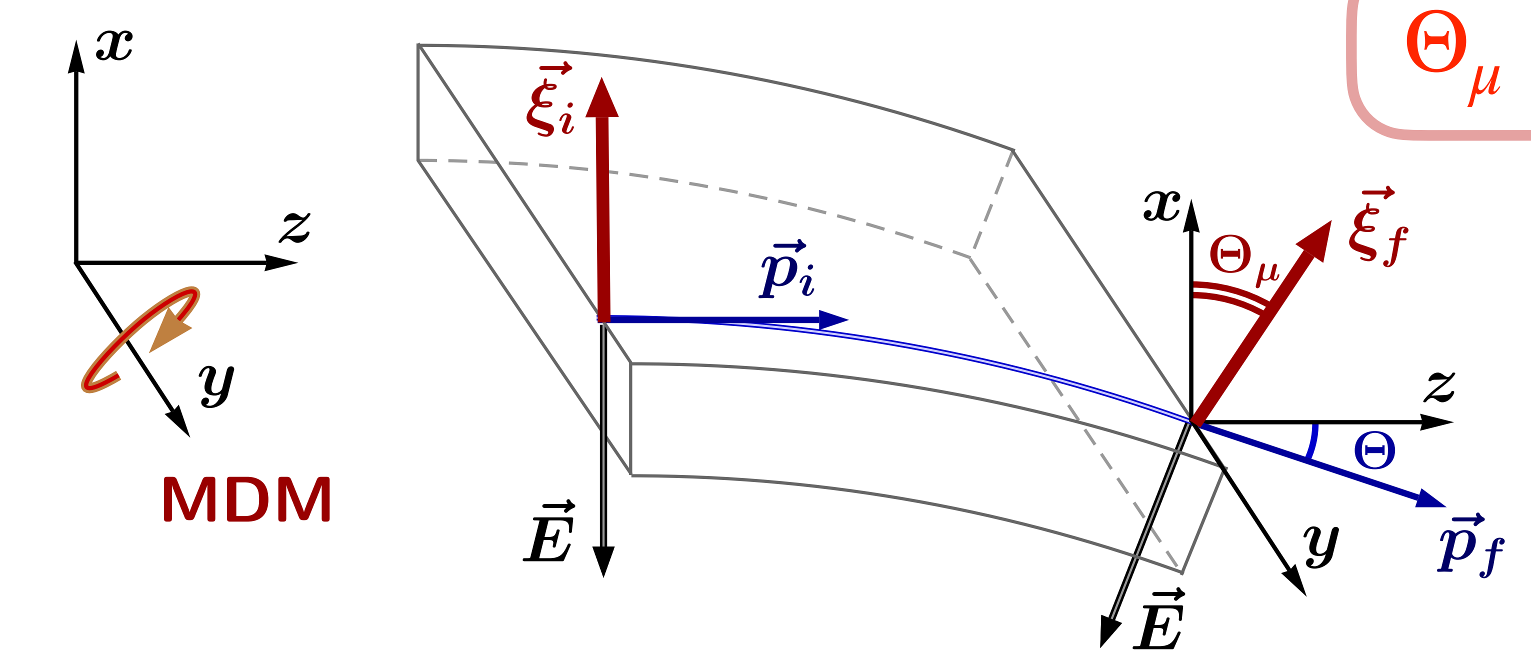

$$\Theta_\mu \equiv \angle(\xi_i \xi_f) = (1 + \gamma a)\,\Theta$$

$$\Delta g = \frac{2}{\alpha \langle \xi_x \gamma \rangle \Theta} \sqrt{\frac{3}{N}}$$

F. J. Botella et al.,
EPJ C77 (2017) 181 [inSPIRE]

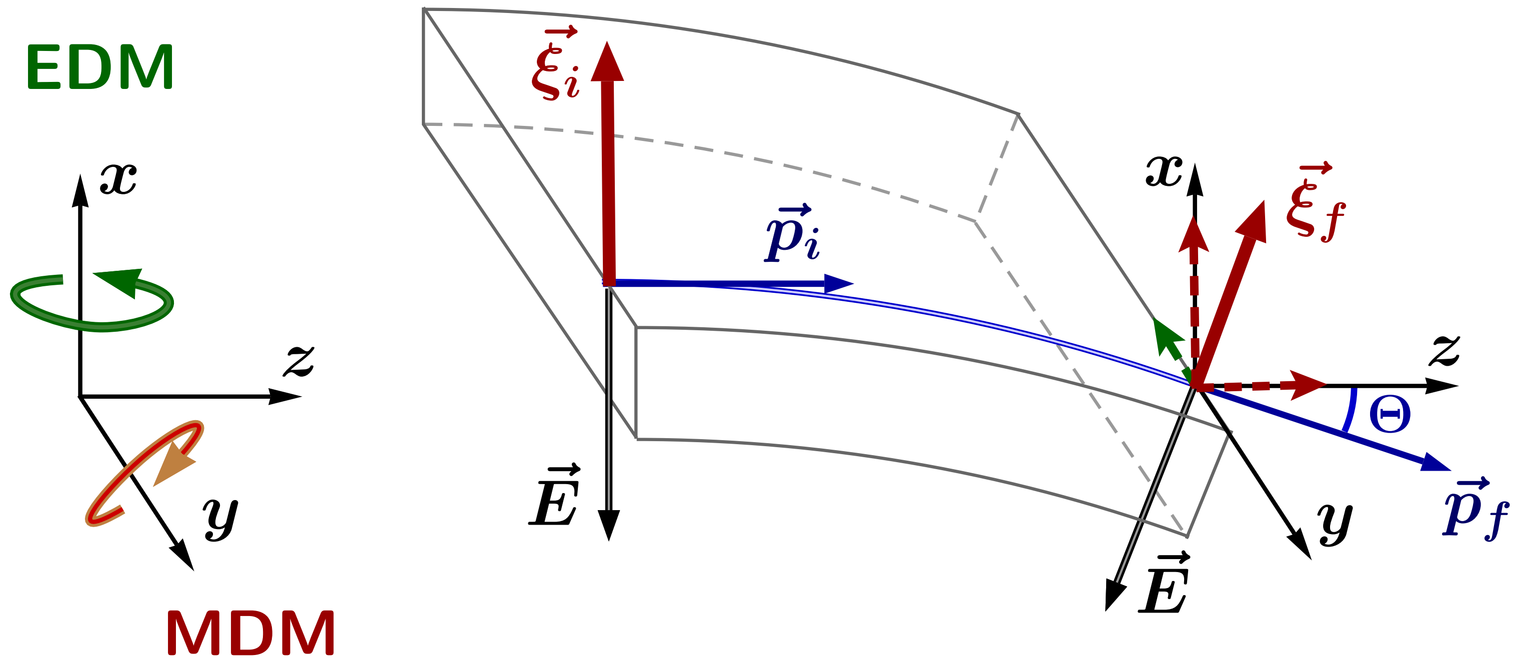

$$\frac{\Delta f}{\Delta g} = \frac{2\,\gamma a}{\Theta\,(1 + \gamma a)^2}$$

V.G. Baryshevsky,
EPJ C79 (2019) 350 [inSPIRE]

A.S. Fomin et al.,
EPJ C80 (2020) 358 [inSPIRE]

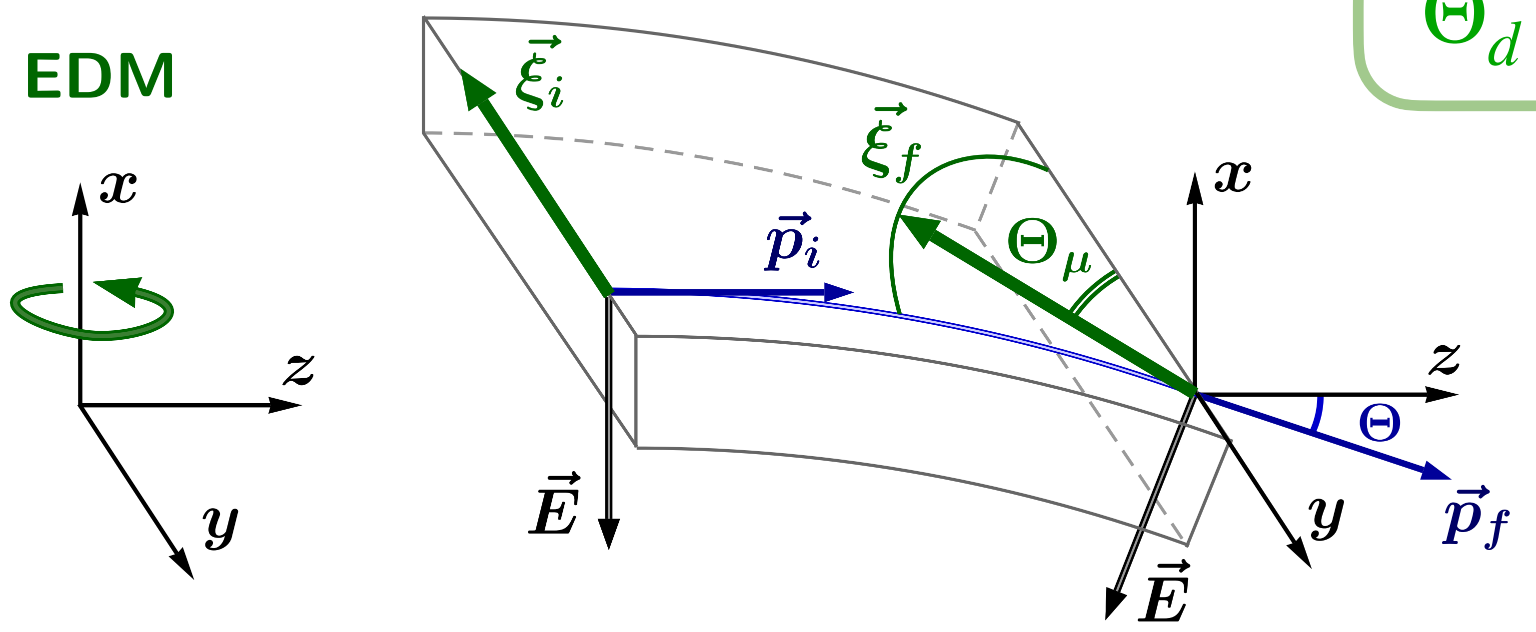

$$\Theta_d \equiv \angle(\xi_i \xi_f) = (1 + \gamma f)\,\Theta$$

$$\Delta f = \frac{2}{\alpha \langle \xi_y \gamma \rangle \Theta} \sqrt{\frac{3}{N}}$$

Optimal crystal orientation for EDM measurement: initial polarisation.

A. Fomin et al. Eur. Phys. J. C (2020) 80:358 [1909.04654]

Production of Λ_c^+ in a fixed target $p + p \to \Lambda_c^+ + X$

Due to the space-inversion symmetry of the strong interaction

Λ_c^+ polarisation is perpendicular to the reaction plane

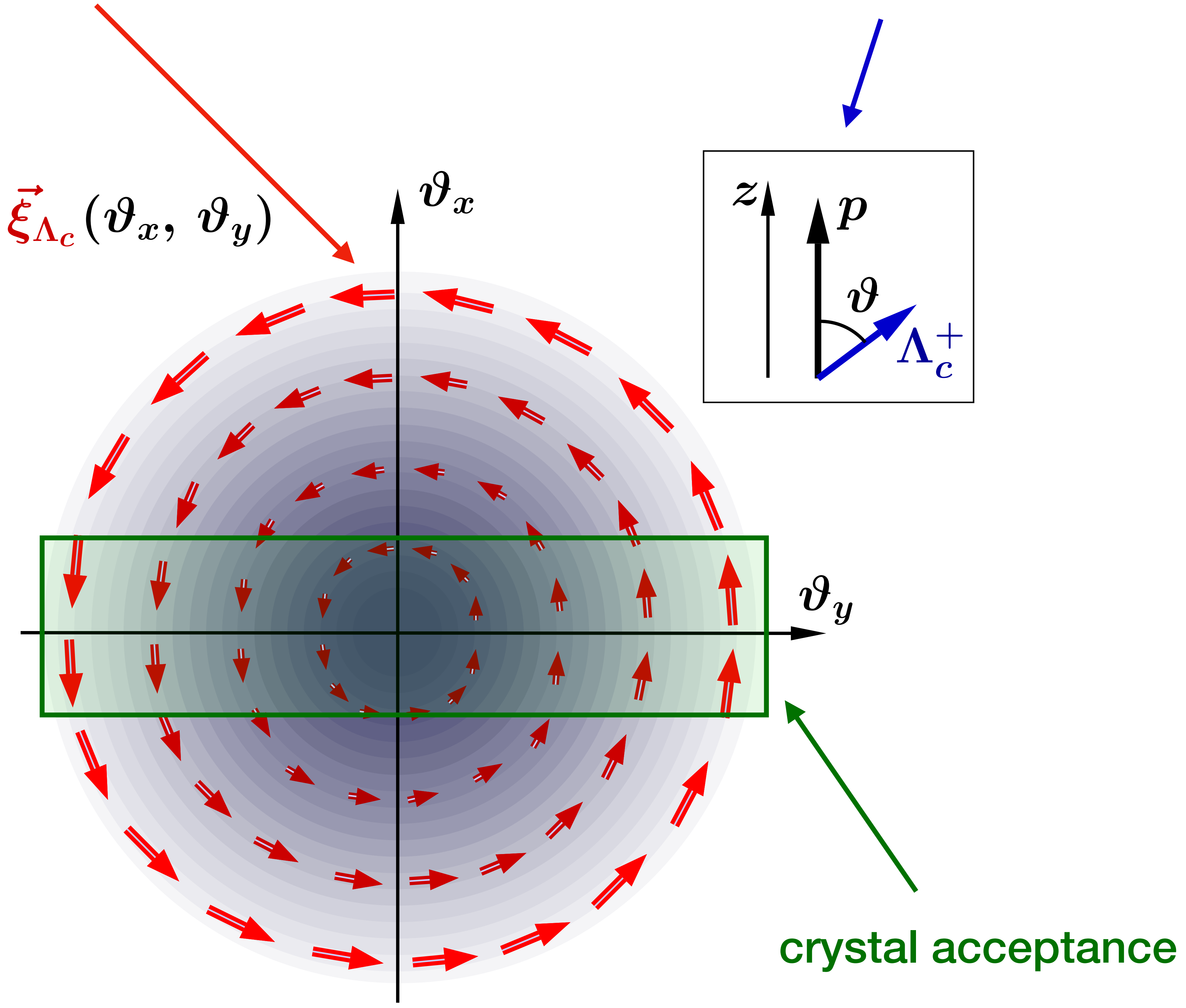

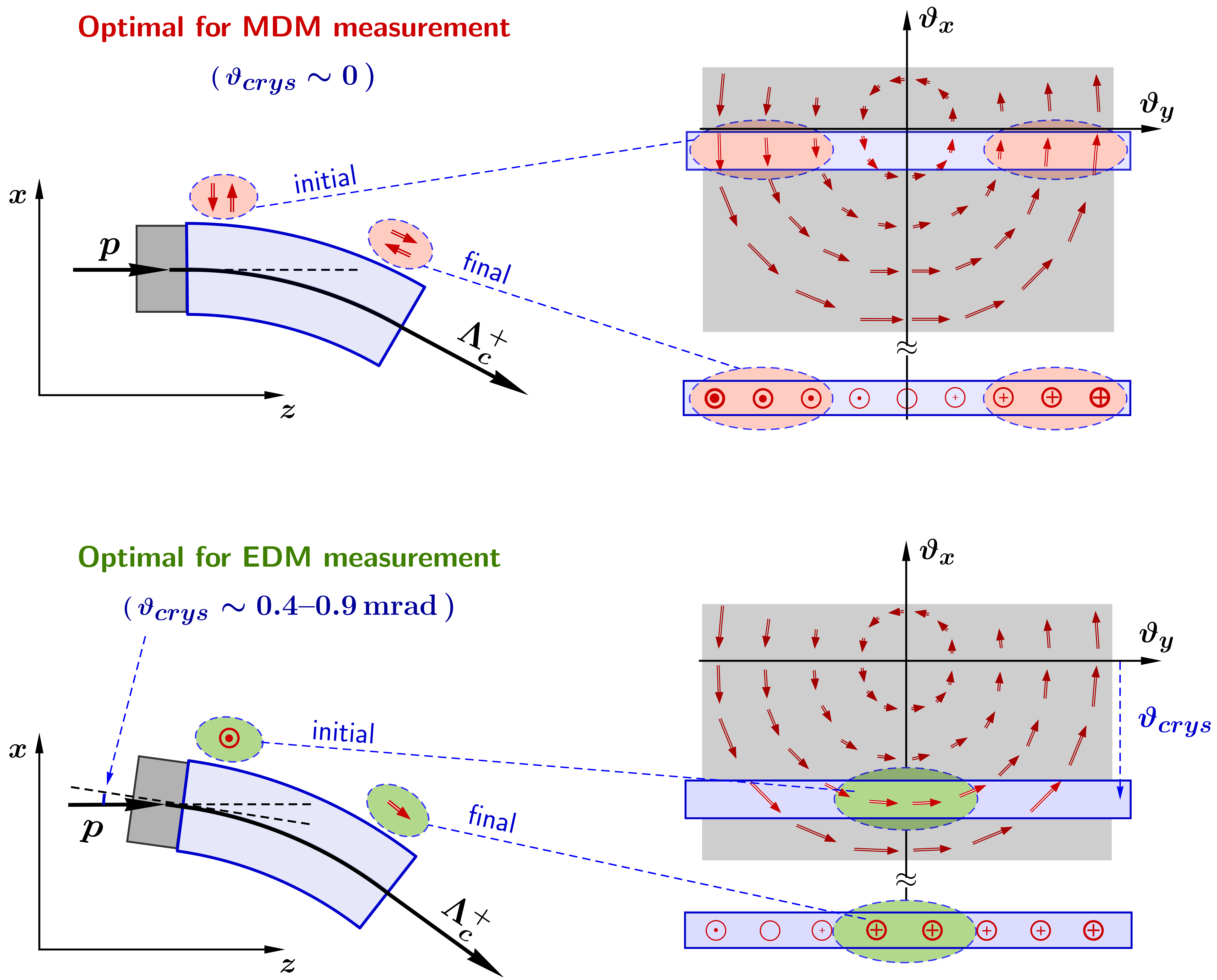

Optimal crystal orientation for EDM measurement: quantitive analysis

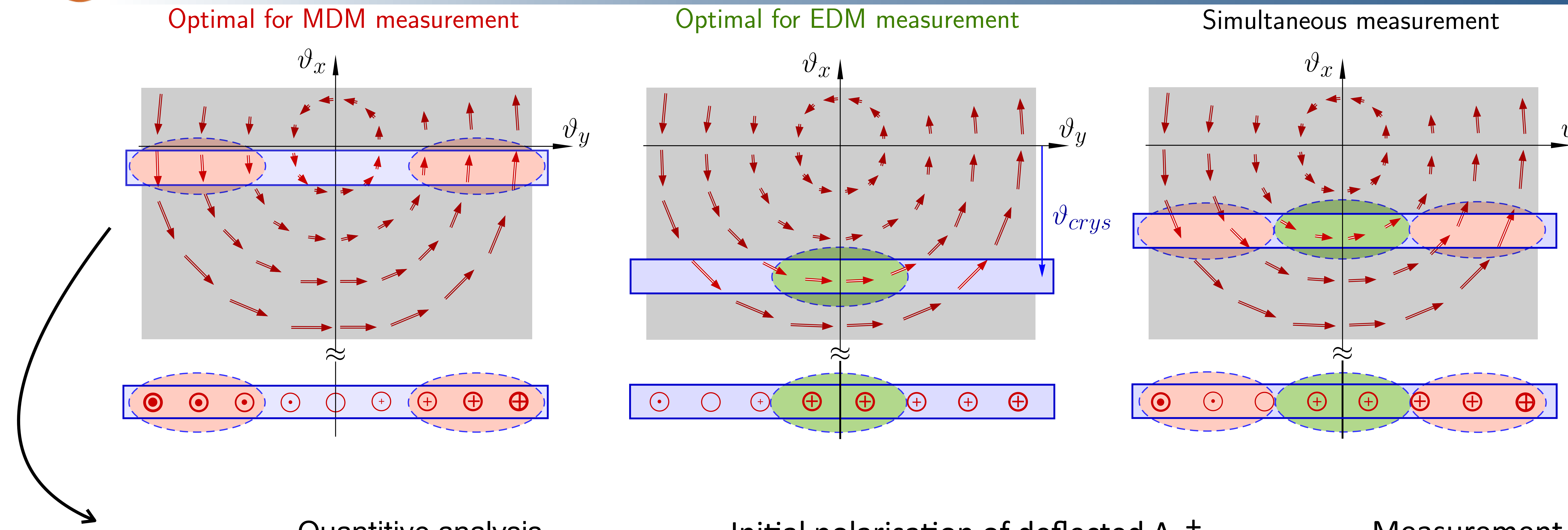

$$\Delta g = \frac{2}{\alpha \langle \xi_x \gamma \rangle \Theta} \sqrt{\frac{3}{N}}$$

$$\Delta f = \frac{2}{\alpha \langle \xi_y \gamma \rangle \Theta} \sqrt{\frac{3}{N}}$$

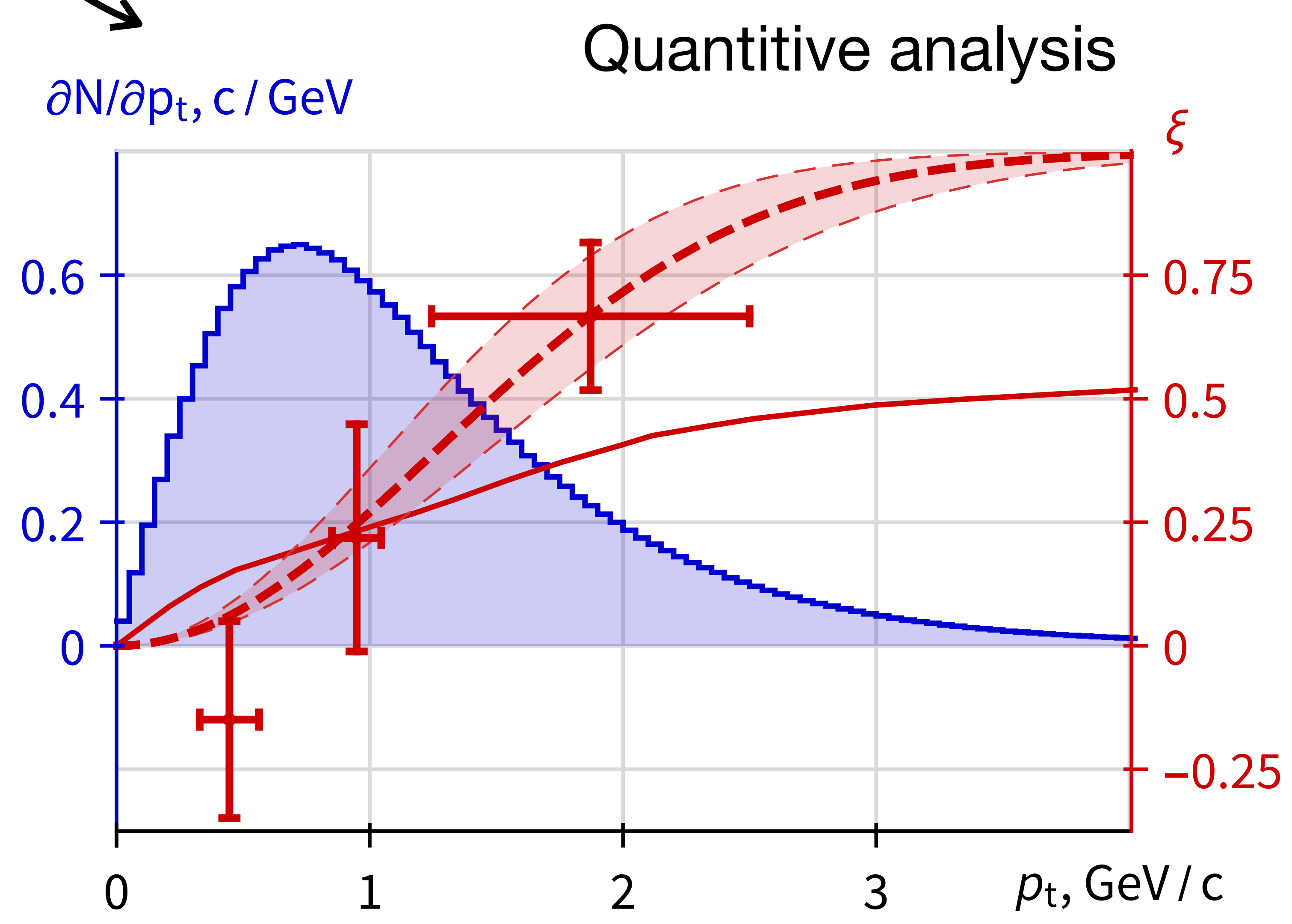

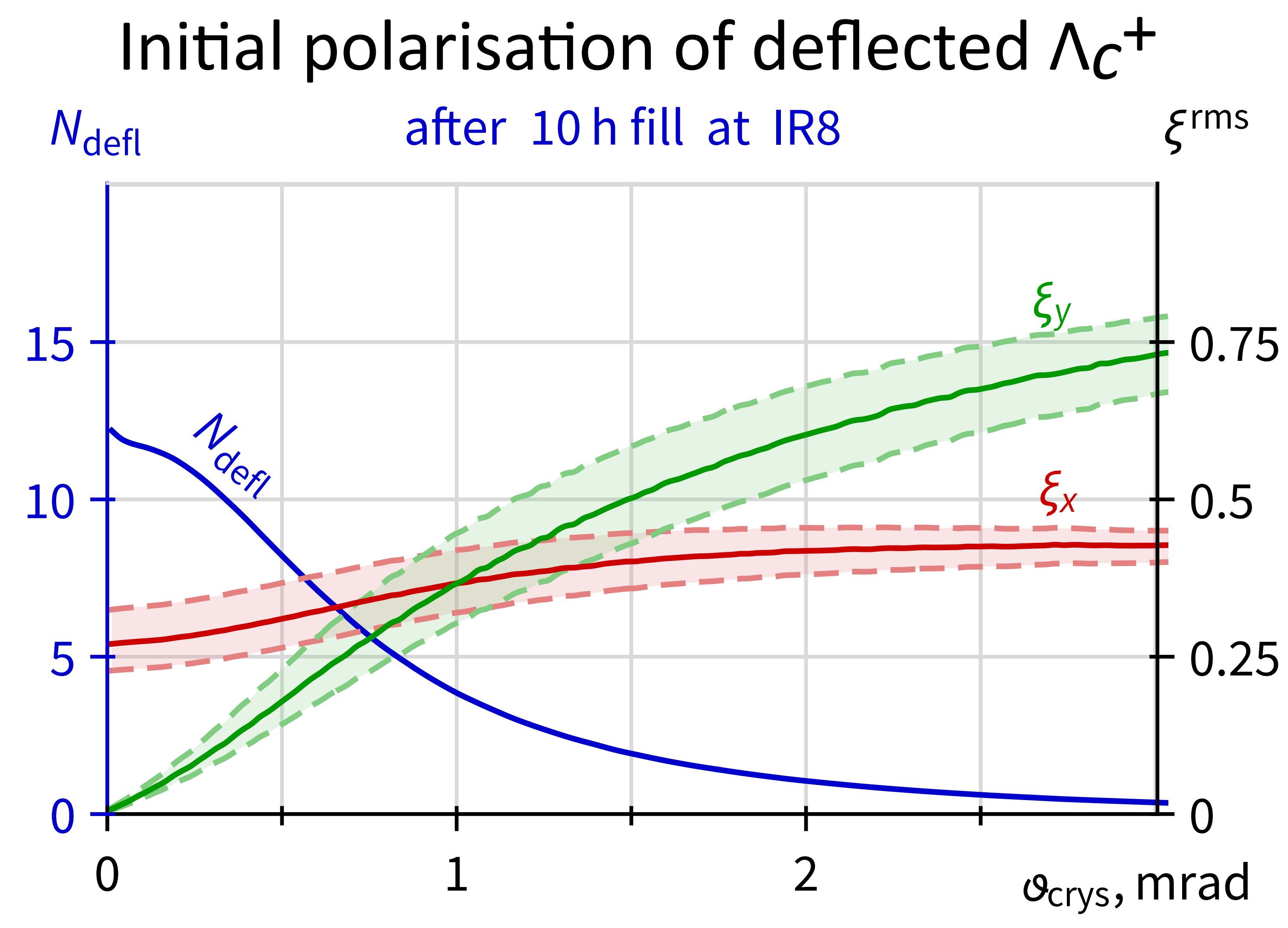

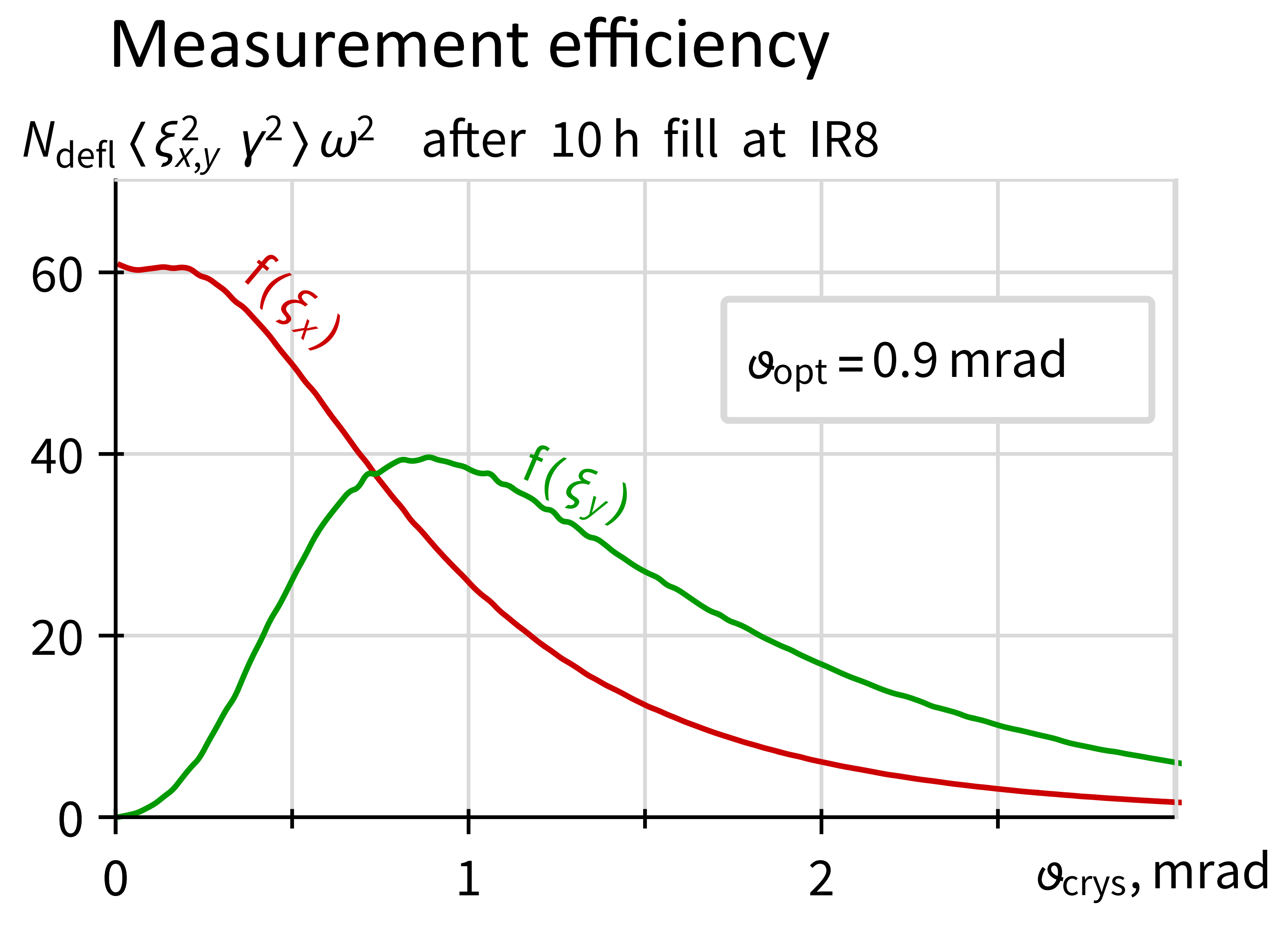

MDM of Σ^+

experiment E761, Fermilab 1990

MDM of Σ+ experiment E761, Fermilab 1990: Mirroring the setup

D. Chen, The Measurement of the Magnetic Moment of Σ+ Using Channeling in Bent Crystals, PhD thesis, SUNY, Albany, 1992.

The main purpose of the experiment was to measure the branching ratio and asymmetry parameter of the Σ^+ radiative decay

A new technique for measuring the magnetic moment of short-lived positively charged particles using channeling in bent crystals was tested.

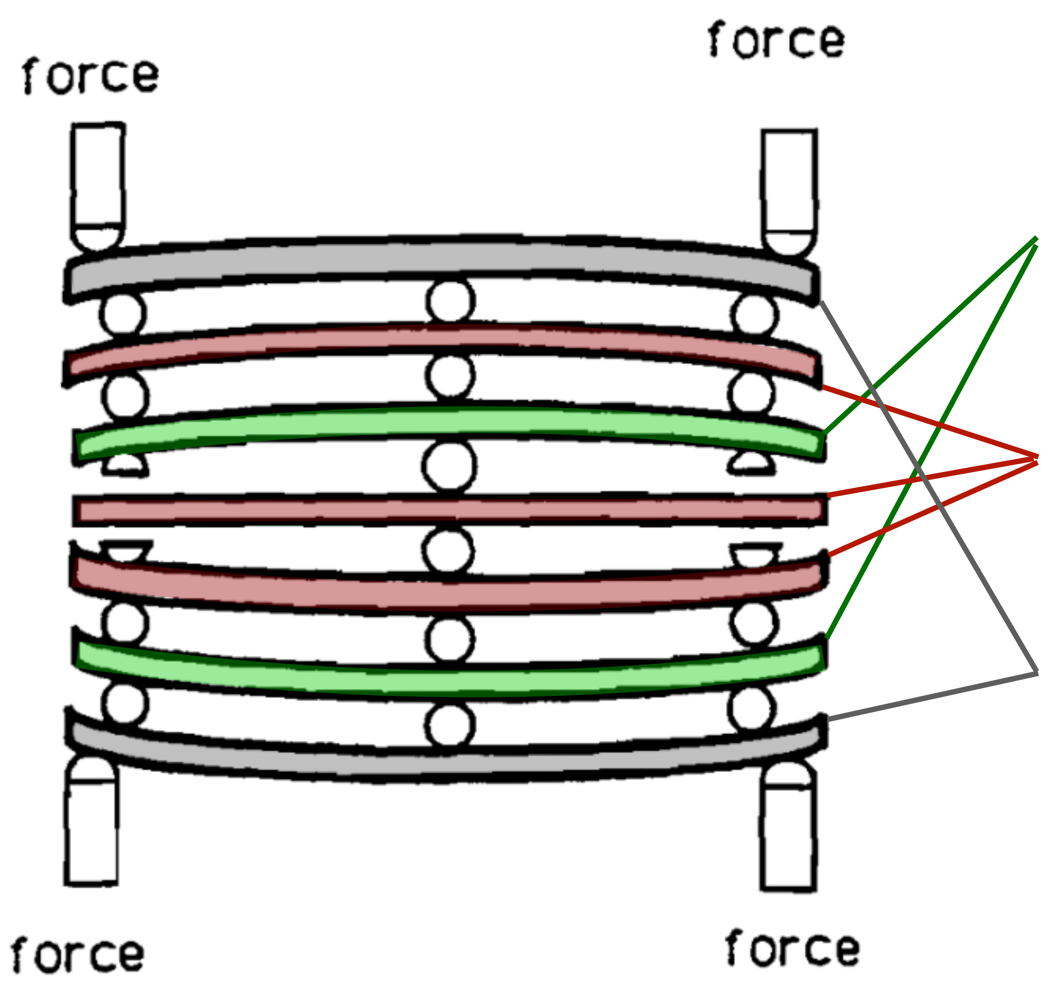

Figure 4.6: Crystal bending device

crystals #2,5 — aligned with the beam

crystals #3,4,6 — **not aligned**

crystals #1,7 — **not in the beam**

After some initial testing, we found that only the **five** center **crystals**, from #2 to #6, were inside the Σ^+ beam phase space in they direction.

Then, during the run, we were only able to align **two** of the five **crystals**, **#2 and #5** with the beam.

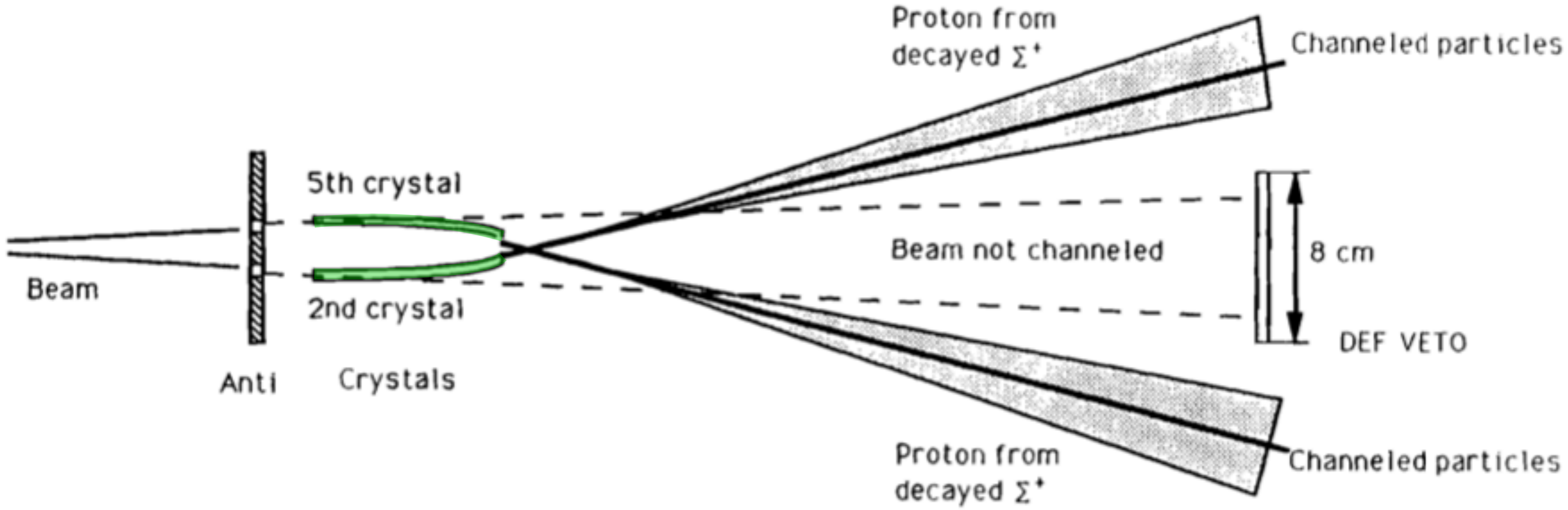

MDM of Σ+ experiment E761, Fermilab 1990: Cancelation of apparatus biases within one crystal

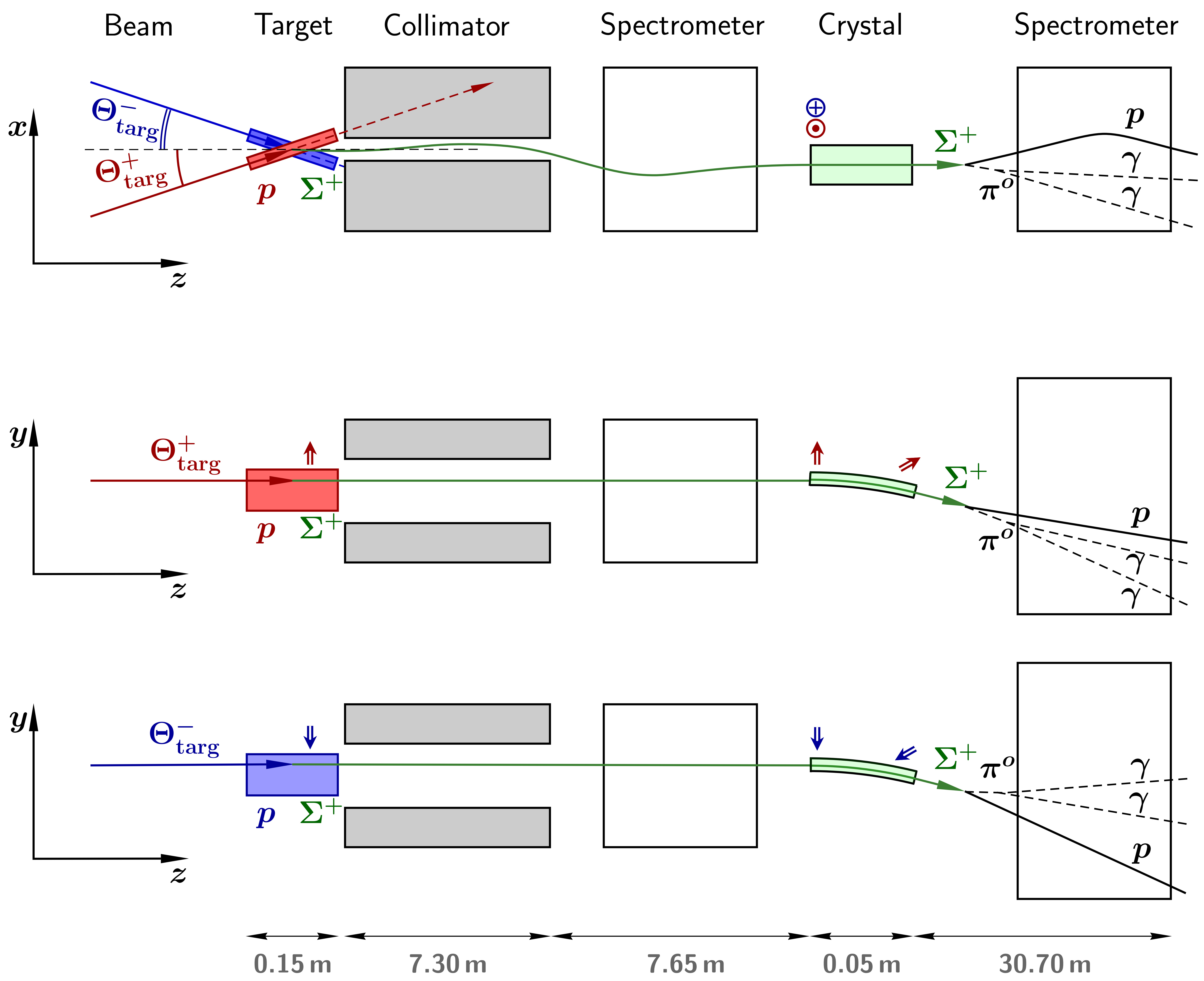

Cancelation of apparatus biases: $\dfrac{N_j^+ - N_j^-}{N_j^+ + N_j^-} = \alpha\, \xi_j^+ \cos\vartheta_j$

$$N_j^+ \equiv \frac{dN_j^+}{N_{0j}^+\, d\cos\vartheta_j} = \frac{Aj(\vartheta_j, \ldots)}{2}\left(1 - \alpha\, \xi_j^+ \cos\vartheta_j\right)$$

more details: [D. Chen, PhD thesis, SUNY, Albany, 1992.]

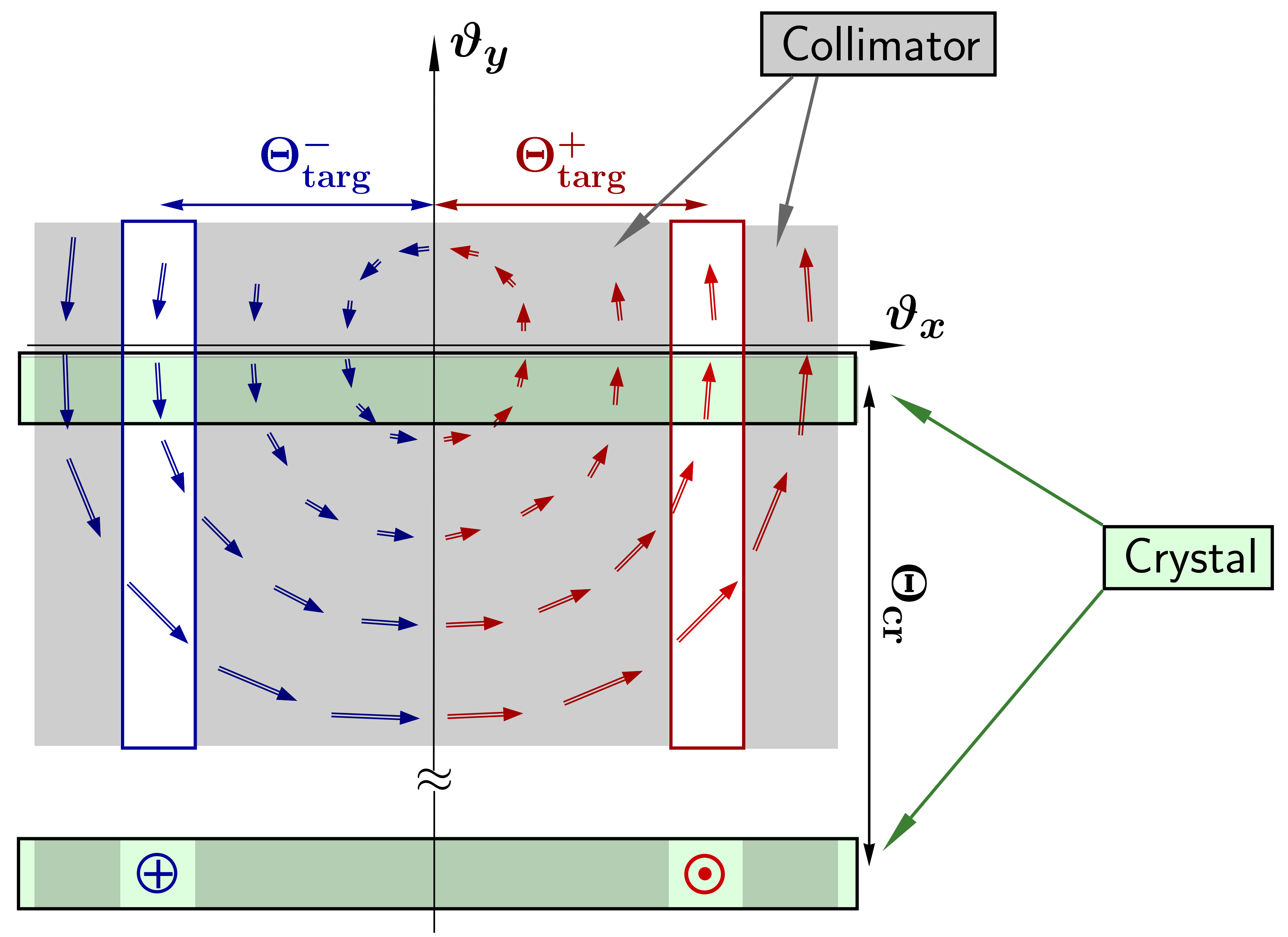

Layouts in IR3 and IR8. Performance assessment

MDM and EDM of charmed baryons: Fixed target at the LHC

- L. Burmistrov et al., CERN-SPSC-2016-030, CERN, Geneva Switzerland, **June 2016** [SPSC-EOI-012].
- A. Stocchi, W. Scandale, talks at Physics Beyond Collider Workshop, CERN, Geneva Switzerland, **6–7 September 2016**.

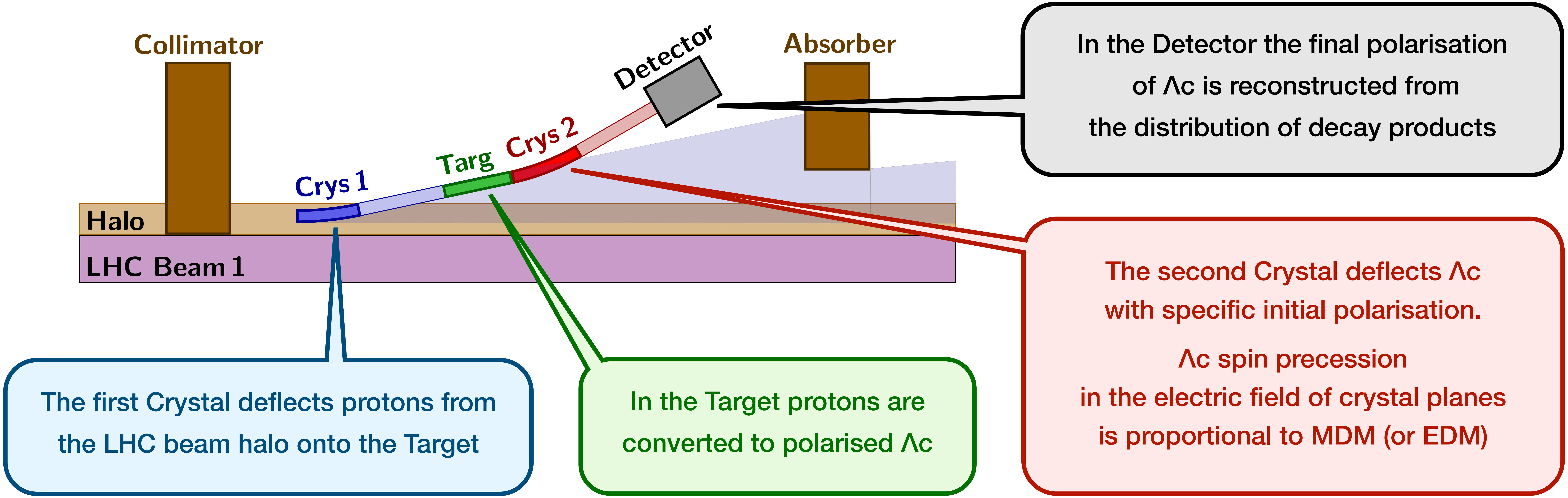

Performance assessment of layouts in IR3 and IR8: precision of measurement

D. Mirarchi et al. Eur. Phys. J. C 80 (2020) 10, 929

- Impact on the machine
- Optimisation of Crystal 1 and Absorbers positions
- Running experiment in a parasitic mode
- Layout in front of LHCb (IR8) 4.3×1010 POT/fill
- Alternative layout at IR3 3.0×1010 POT/fill
- Restriction on Crystal 2 bending radius

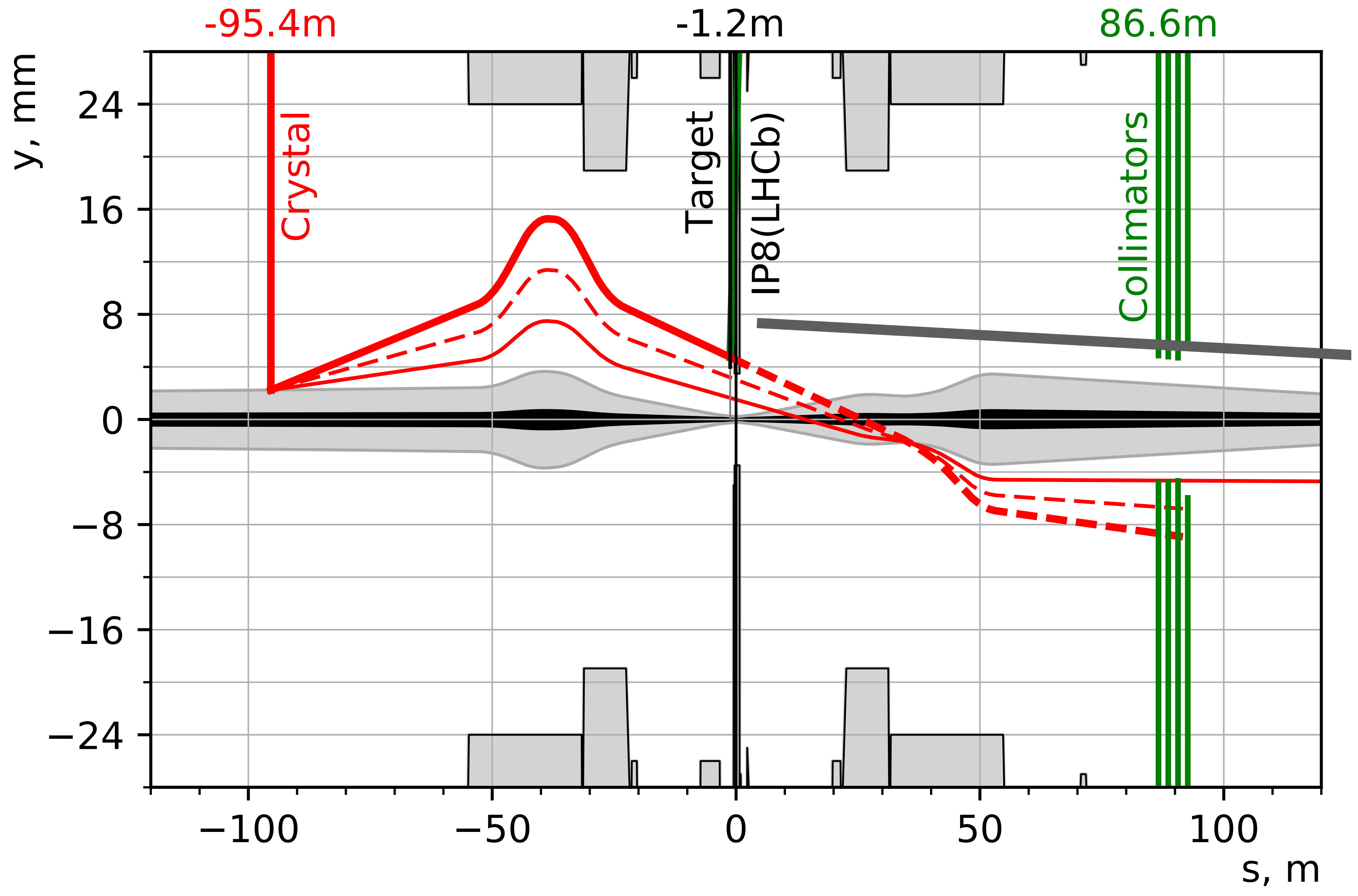

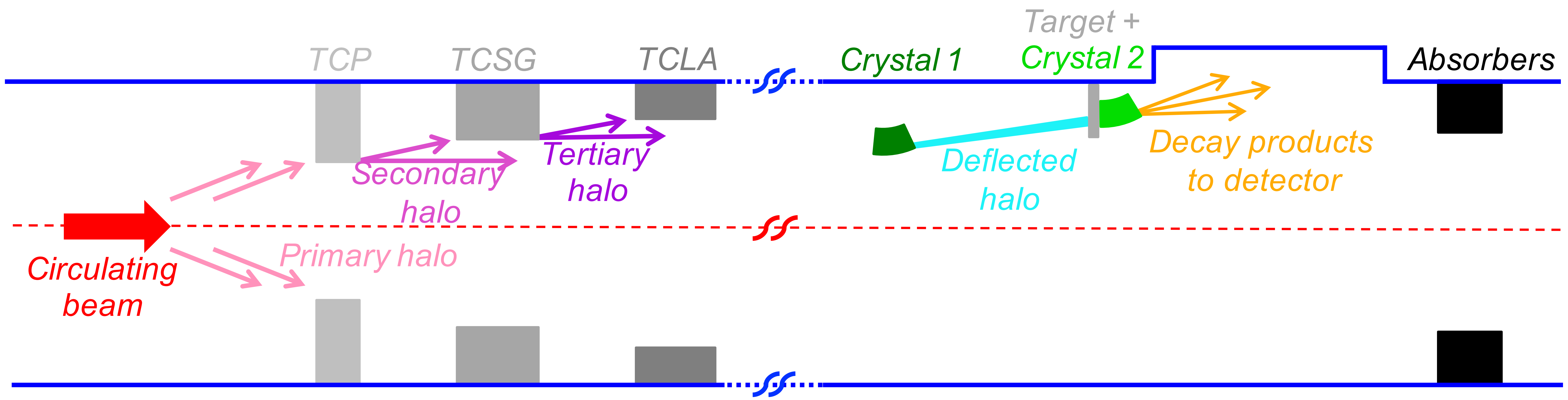

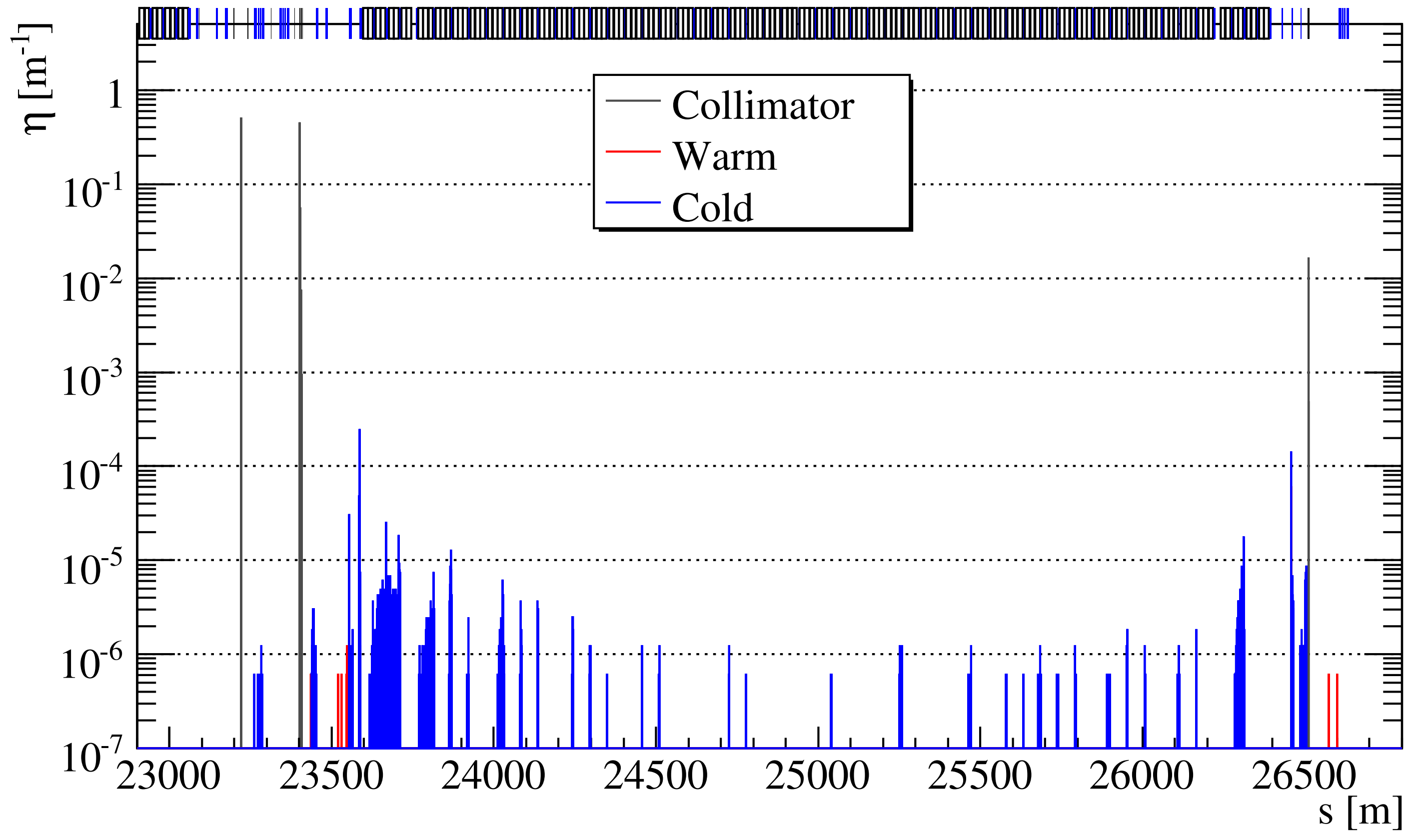

Performance assessment of layouts in IR3 and IR8: precision of measurement

A. Fomin et al. Eur. Phys. J. C (2020) 80:358 [1909.04654]

Layout		IR3	LHCb
Target	proton rate, 10^{10} per 10h fill	3*	4.3*
	length, mm	5	5
Crystal	length, mm	70*	75**
	bending radius, m	14*	5.4**
	deflection angle, mrad	**5**	**14**
Λ_c^+	Average Lorentz factor	**1140**	**600**
	Weighted average polarisation	0.22(5)	0.26(5)
	deflected per 10h fill	**180**	**12**
	relative precision of MDM	**1**	**2.7**
	relative data taking time	**1**	**7.5**

* D. Mirarchi et al. Eur. Phys. J. C 80 (2020) 10, 929

** E. Bagli et al., EPJ C77 (2017) no.12, 828

$$\Delta g = \frac{2}{\alpha \langle \xi_x \gamma \rangle \Theta} \sqrt{\frac{3}{N}}$$

Thorough evaluation of initial polarisation of channeled Λ_c^+

- Spectra-angular distribution of Λ_c^+ (Pythia 8.243)
- Channeling probability as a function of Λ_c^+ energy, bending radius and length of the crystal
- Initial polarisation of Λ_c^+ as a function of transverse momentum

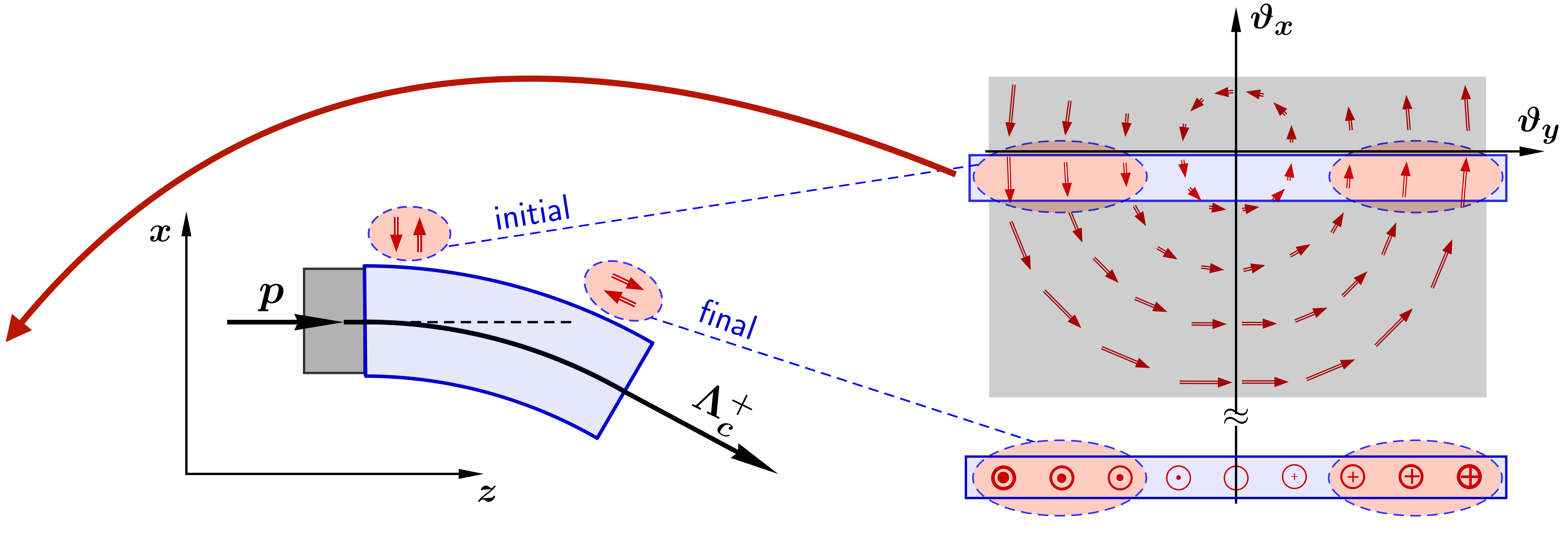

The error of g-factor Δg is calculated considering:

- Detector at IR3 would have the same resolution as LHCb for higher energies, and angular acceptance ≥ 5 mrad
- Systematical error from poor knowledge of α and ξ

Active bunch excitation

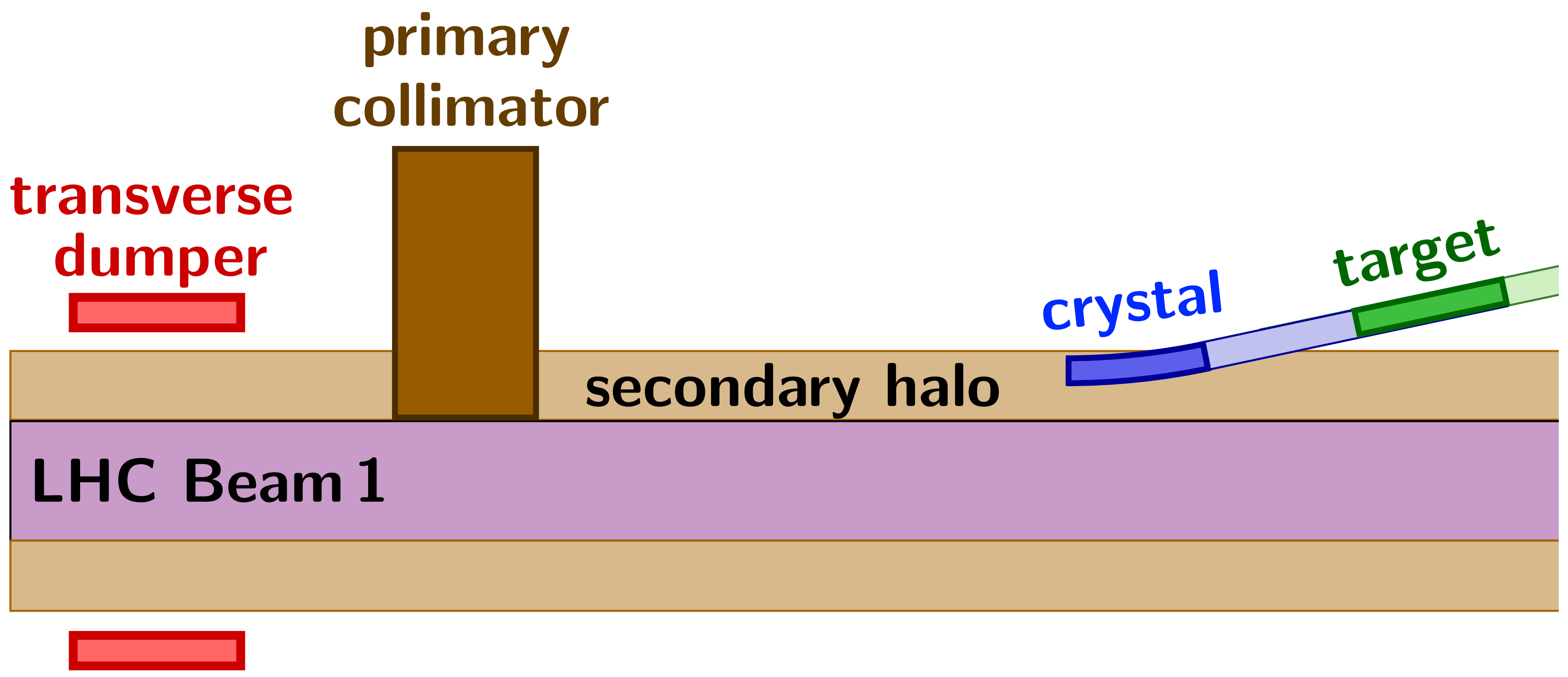

General idea

- apply random noise excitations with the **transverse damper** when a selected trains of bunches pass by

→ **emittance grow** of these bunches

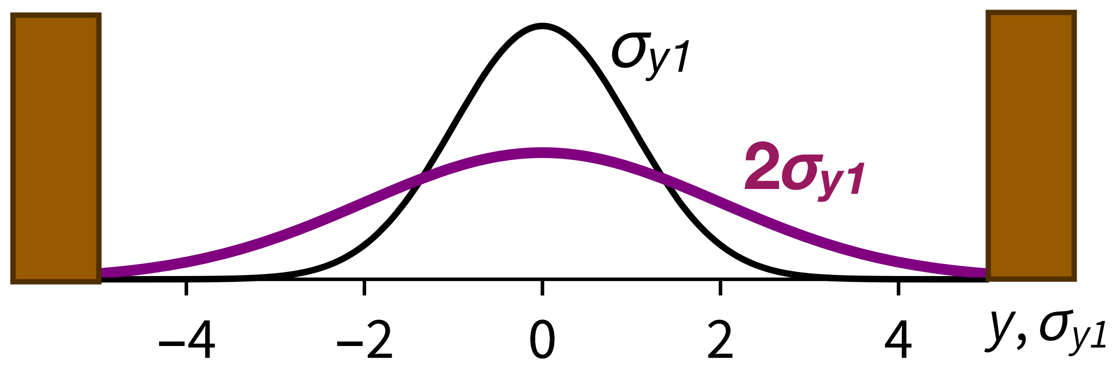

→ increase the loss rate in **primary collimators** at IR7

→ enrich the **secondary halo** of the beam

→ increase the flux on the **crystal** → increase the deliverable rates of **PoT**

Transverse damper is currently used in LHC

- corrects the trajectory of the bunches during the fill
- increase the loss rate during alignment of collimators

Drawback — reduction of total luminosity

- excitation during the fill → higher emittance
- excitation before dumping → longer turn-around time

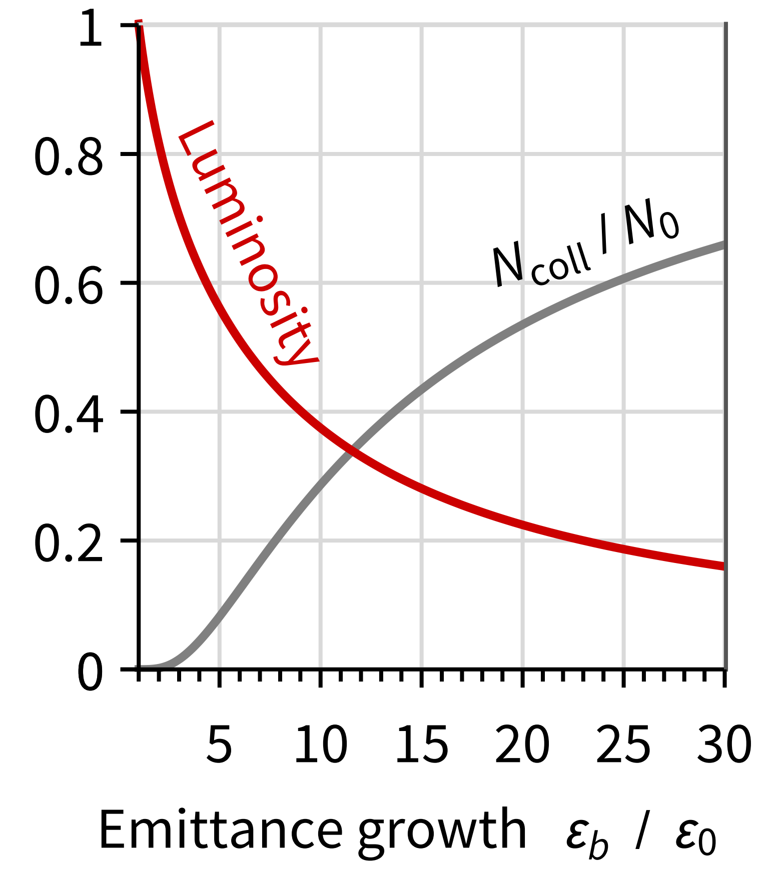

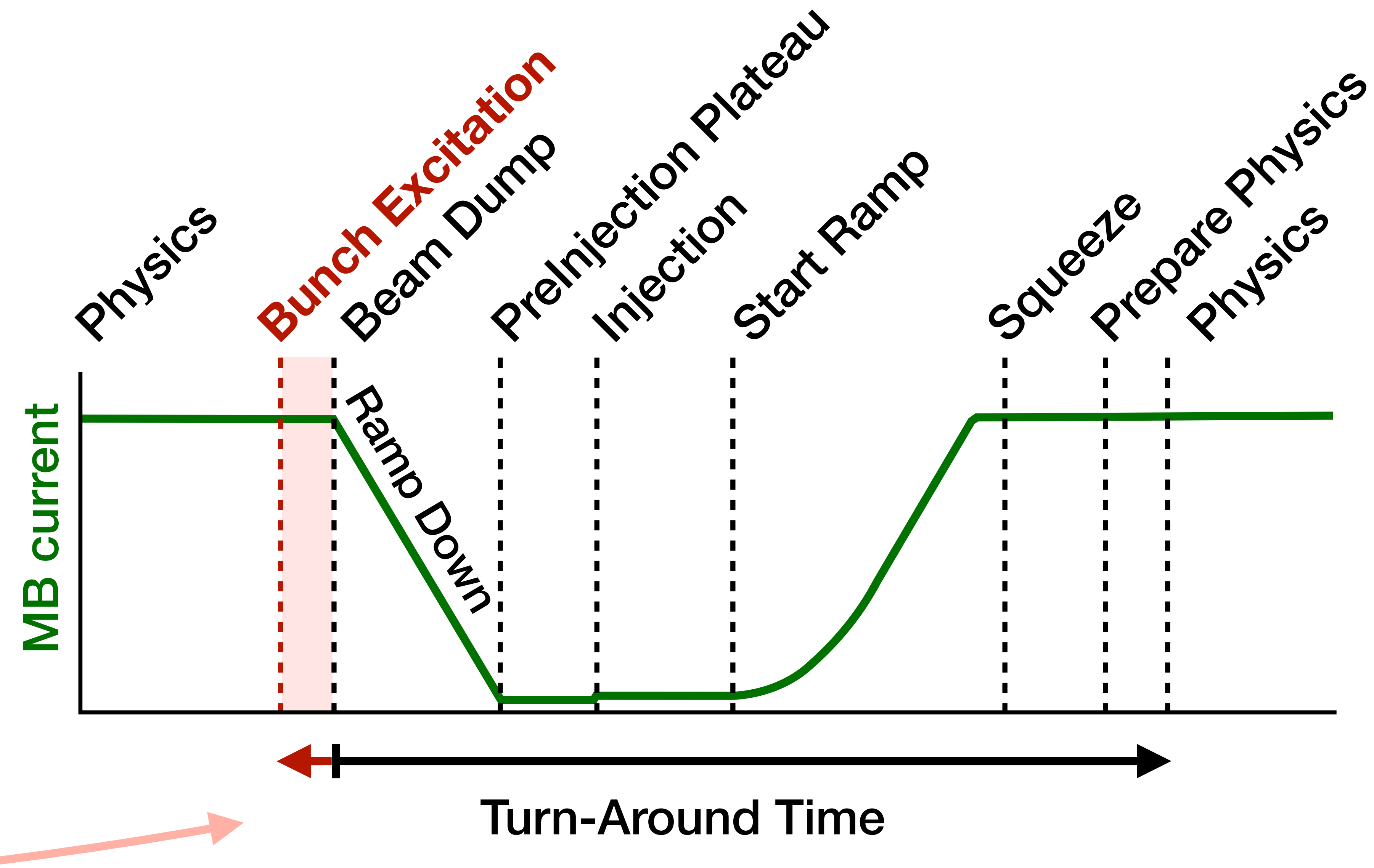

Maximum achievable PoT due to beam excitation (based on 2018 run data)

The gain factor in PoT from the beam excitation
with respect to the “Baseline” (no excitation):

$$\eta_{exc} = \frac{N_{PoT}^{(ex)}}{N_{PoT}^{(BL)}}$$

too high rates of PoT per bunch crossing (~49 @LHCb)

					200 kW in coll. system		3.5 p / bunch X @ LHCb		
					after collisions			after collis.	during collis.
Beam excitation	N_{coll}	N_{PoT} (IR3)	N_{PoT} (IR8)	η_{exc}	*t, h*	*ΔL / L*	t, h	$\Delta L / L$	$\Delta L / L$
No excitation (“Baseline”)	$1.7{\times}10^{15}$	$4.7{\times}10^{12}$	$6.8{\times}10^{12}$	1	*1908*	*0*	1908	0	0
All fills, no limit on Δt	$4.7{\times}10^{15}$	$2.6{\times}10^{13}$	$3.8{\times}10^{13}$	5.6	*8*	*> 0.4 %*	167	8.7 %	2.9 %
Selected fills (2556b), Δt < 1 hour	$2.5{\times}10^{15}$	$1.4{\times}10^{13}$	$2.0{\times}10^{13}$	3.0	-	-	54	2.8 %	1.2 %

The most efficient scenario:

The gradual excitation of bunches (3.5 p/bunch X) at the end of the fills with 2556 bunches, with duration under 1 hour:

⇒ delivers **3 times more PoT** w.r.t. “Baseline”

⇒ reduces the total luminosity at ATLAS and CMS by **~1.2%**

Performance assessment of layouts in IR3 and IR8: possible improvements

A. Fomin et al. EPJ C80 (2020) 358

- Thicker target 5 mm → 40 mm: ionisation energy losses and multiple scattering can be neglected, showers production - to be checked
- Proton rate, 3–4.3×10^{10} per 10h fill
  D. Mirarchi et al. EPJ C80 (2020) 10, 929

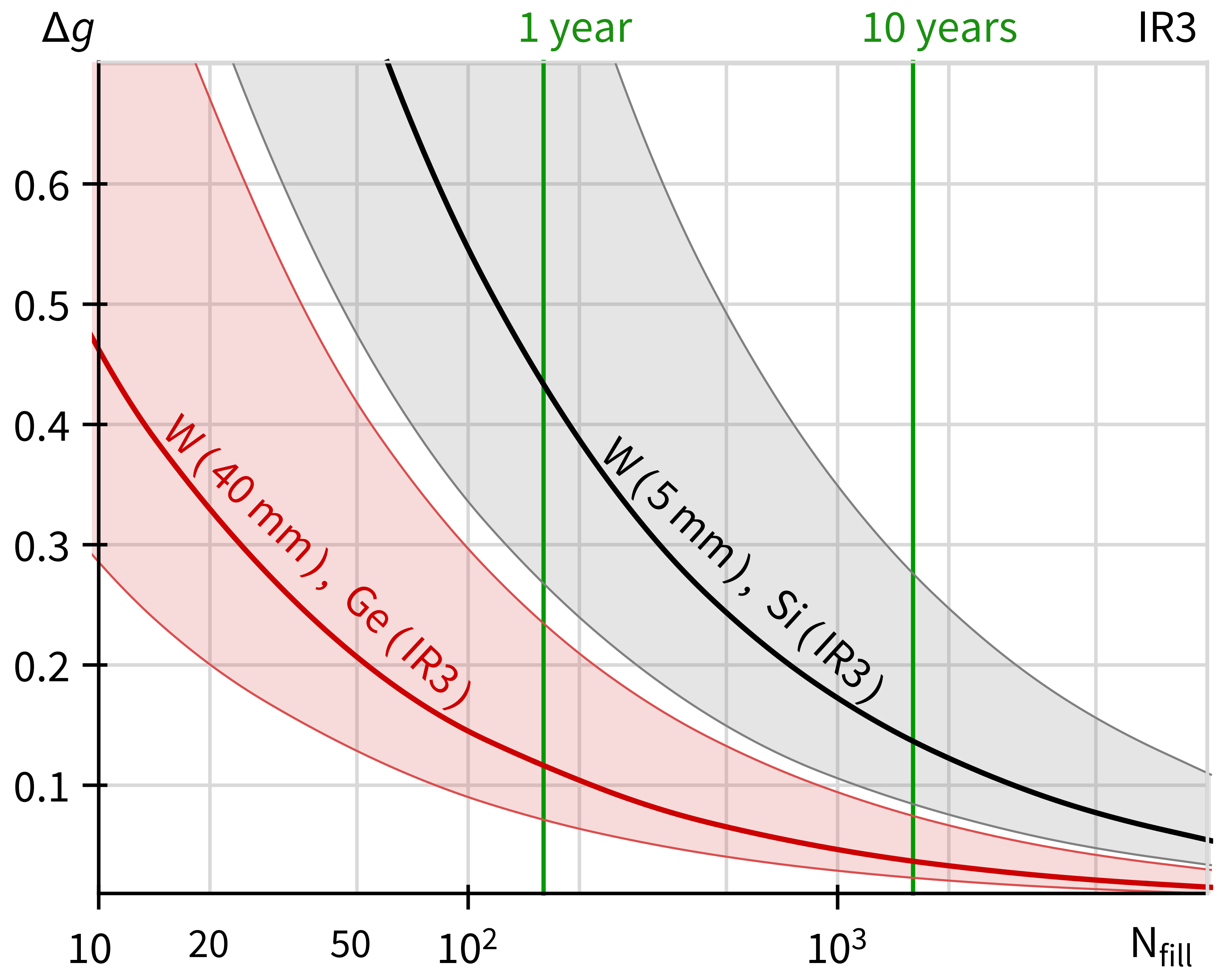

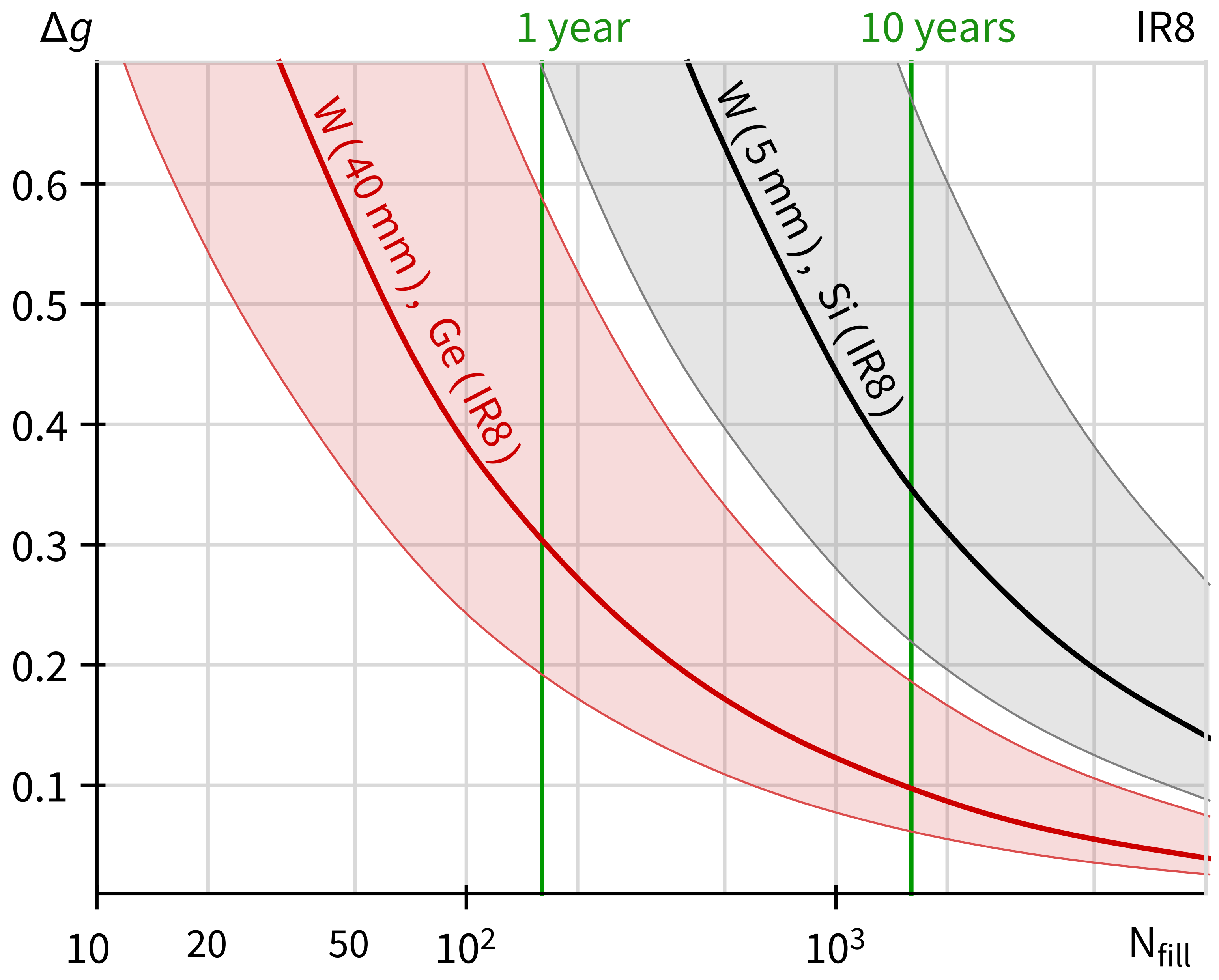

Possible improvements:

	1 → 2	**t1/t2**
Target	5 mm → 40 mm	**6**
Crystal	silicon → germanium	**2.4**
Detector	LHCb (IR8) → dedicated at IR3	**7.5**

Bunch excitation — up to **3 times** more PoT

- **10 year** at **LHCb**, ~7×10^{13} POT, **5mm**, **Si** → Δg ~ **0.35**
- **1 year** at **IR3**, ~0.5×10^{13} POT, **40mm**, **Ge** → Δg ~ **0.12**
- big uncertainty (×10) due to α parameter

Conclusions & Outlook

Initial polarisation in double crystal setup

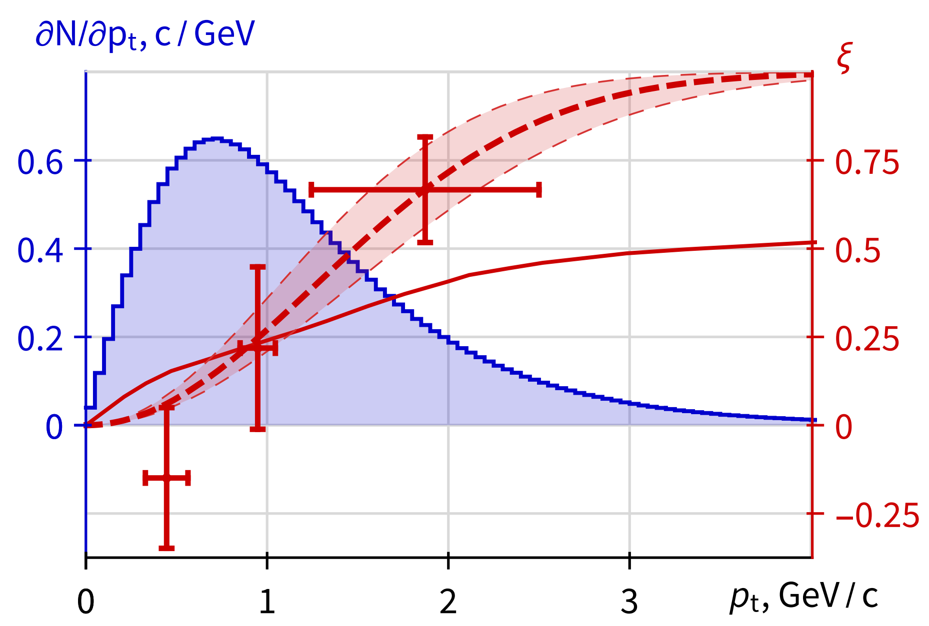

- new corrected value of initial polarisation of channeled Λ_c^+: 0.22(5) and 0.26(5) for IR3 and LHCb

Performance assessment of layouts in IR3 and IR8

- dg=0.35 (LHCb) and dg=0.14 (IR3) after 10 years
- 5 mm → 40 mm ~ **6** time reduction
- silicon → germanium ~ **2.4** time reduction
- LHCb (IR8) → dedicated at IR3 ~ **7.5** time reduction

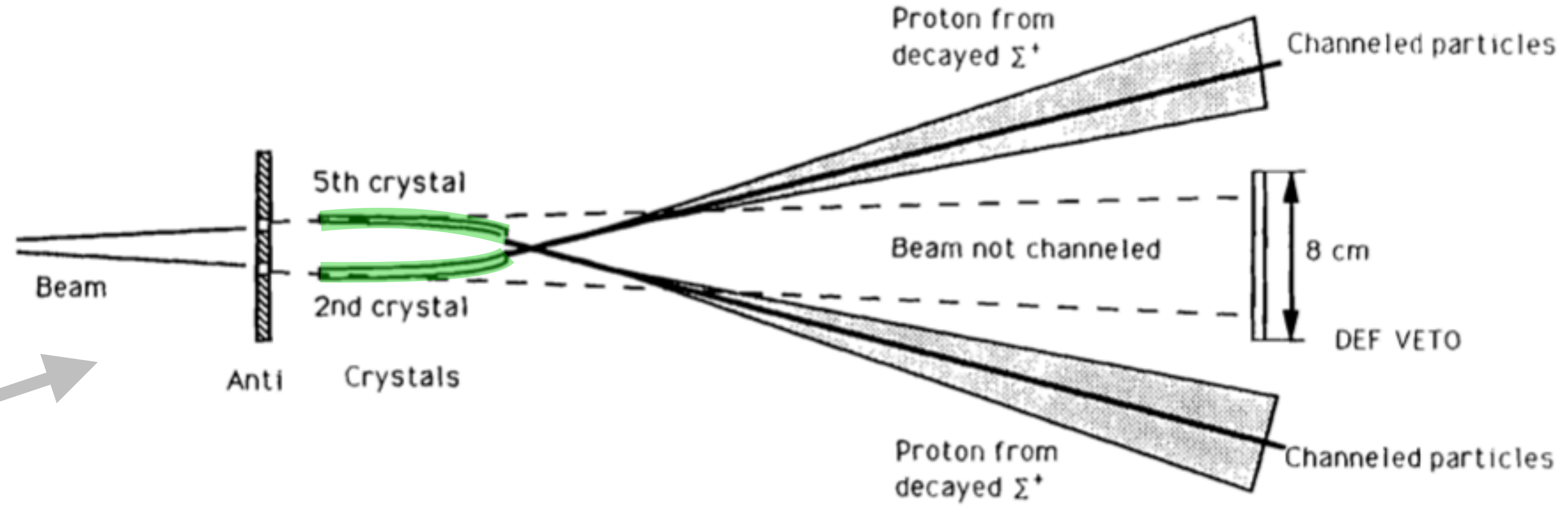

MDM of Σ+ (experiment E761, Fermilab 1990)

- Mirroring the setup — doubling the statistics

Optimal crystal orientation for EDM measurement

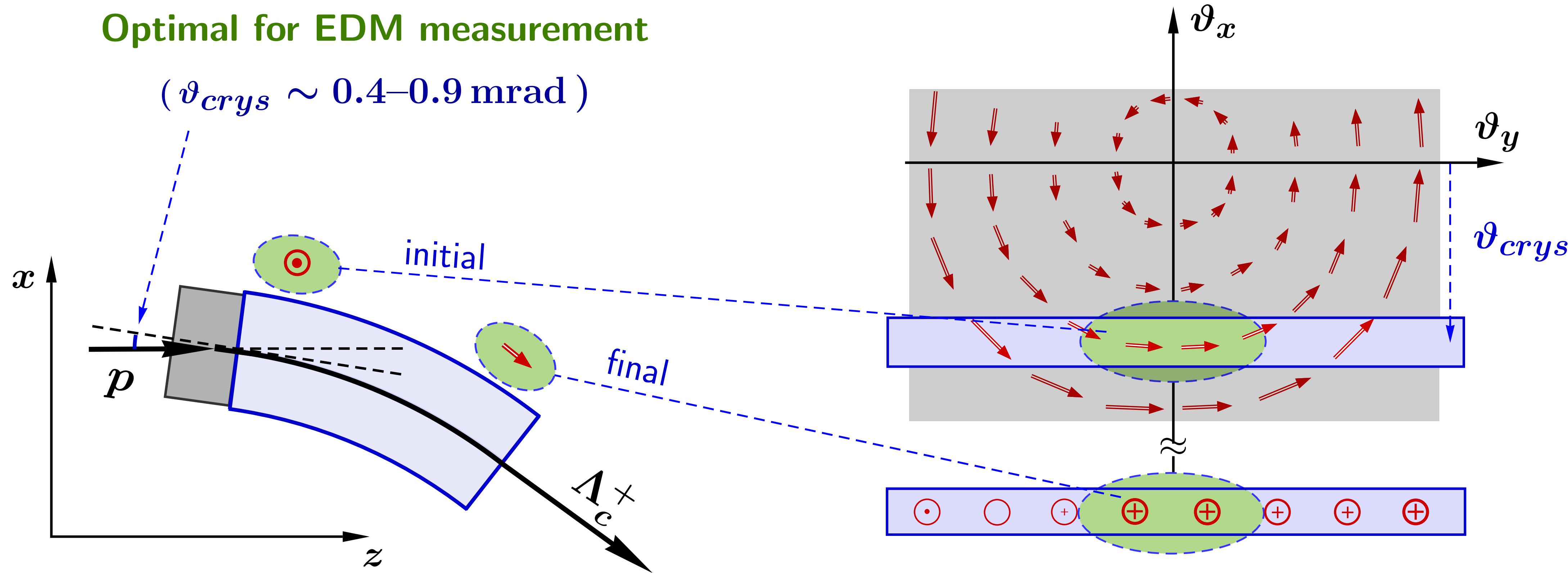

- slight tilt around bending axis ~ 0.9 mrad (for LHCb)
- data taking time reduced by ~170
- 10 years at IR8, 40mm, Ge, $\Delta d \sim 2.6\ 10^{-16}$ e cm

Outlook

Polarisation of Λc (from SMOG data)

- initial polarisation as a function of transverse momentum
- reconstruction of final polarisation

Crystals in circulating machines

- channelling of secondary halo in the LHC
- double channelling scheme proved at SPS (2018)

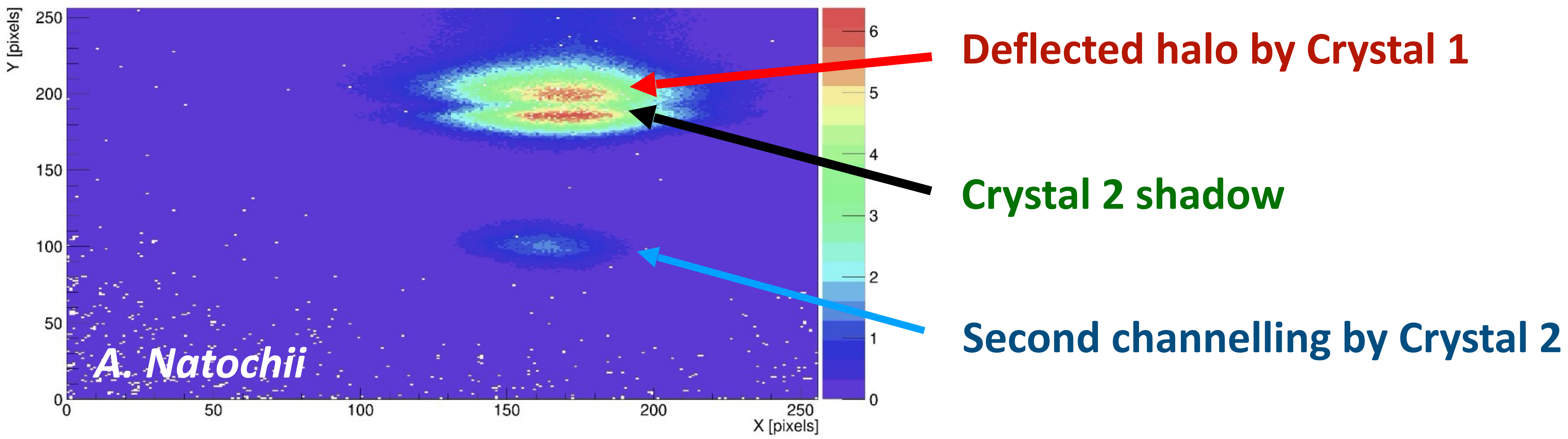

Long crystal channeling efficiency

- UA9 at H8 180GeV
- SELDOM at H8 180GeV   Si(111), 8cm, 5m; Ge(110) 5.5cm, 3.7m
- simulations vs experiment
- extrapolation to TeV energies

Considerations for the layouts in LHC

- Mirroring the setup — doubling the statistics
- Channeled halo and new VELO aperture
- Dynamic changes during levelling at IR8
- Increasing the statistics of the LHC fixed-target experiments through bunch excitation

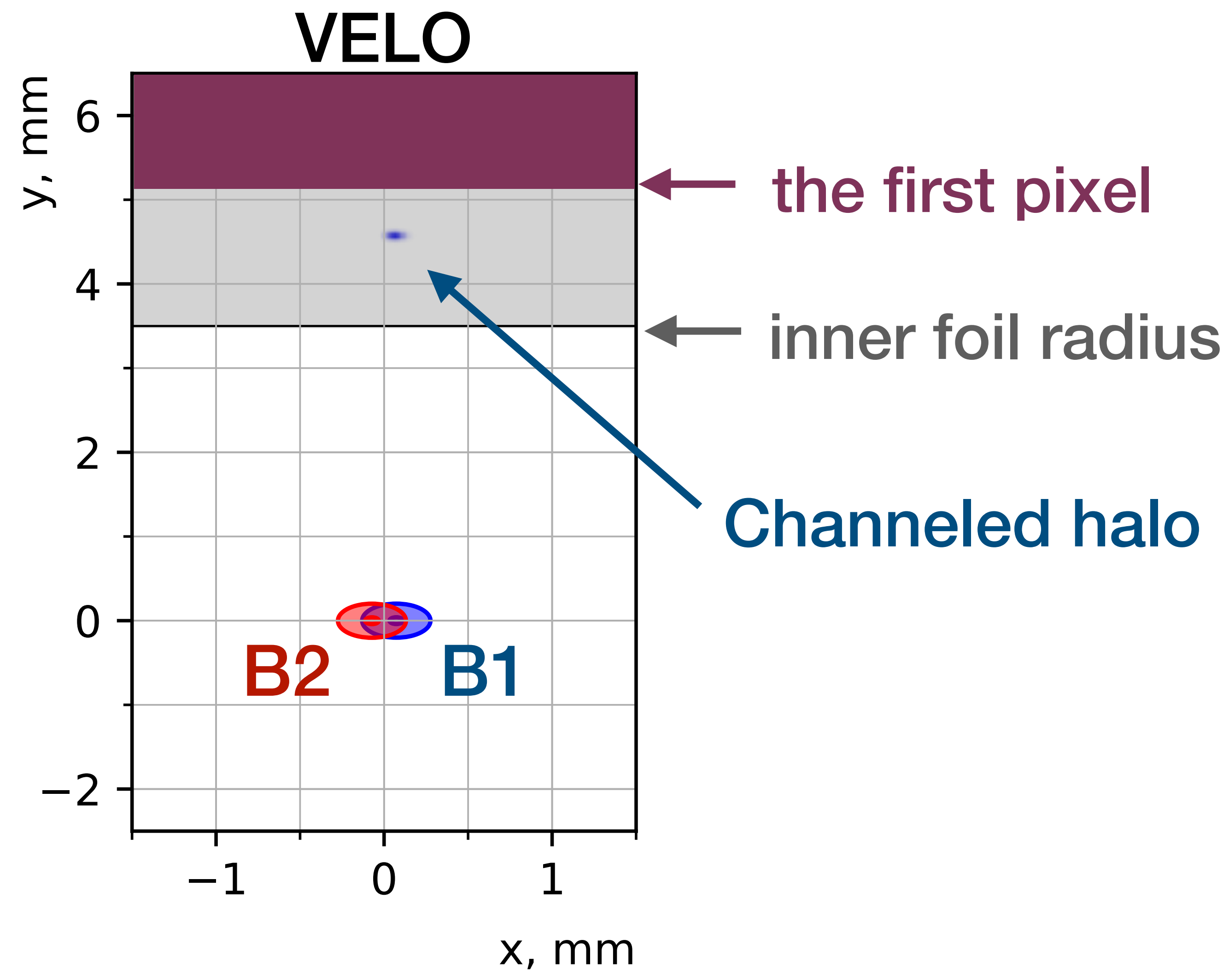

Magnetic dipole moment (MDM) of τ *(LAL 2017 – 2018)*

$$p\,p \to D_s^+ \ldots \to \tau^+ \ldots \to 2\pi^+\pi^- \ldots$$

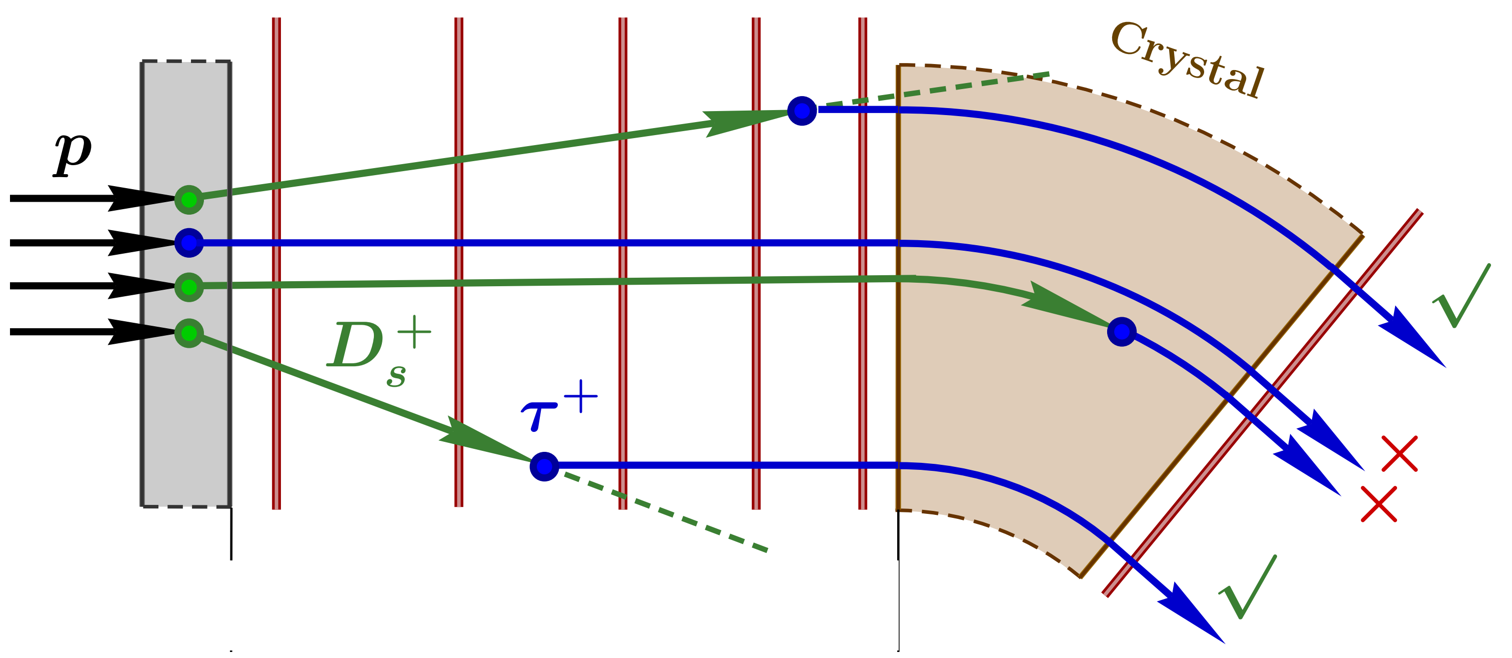

First proposal for measuring the MDM of τ-lepton using crystals

- studied initial polarisation of τ-lepton from Ds decay
- two layouts: with Tracker & with additional Crystal (less background, greater P)

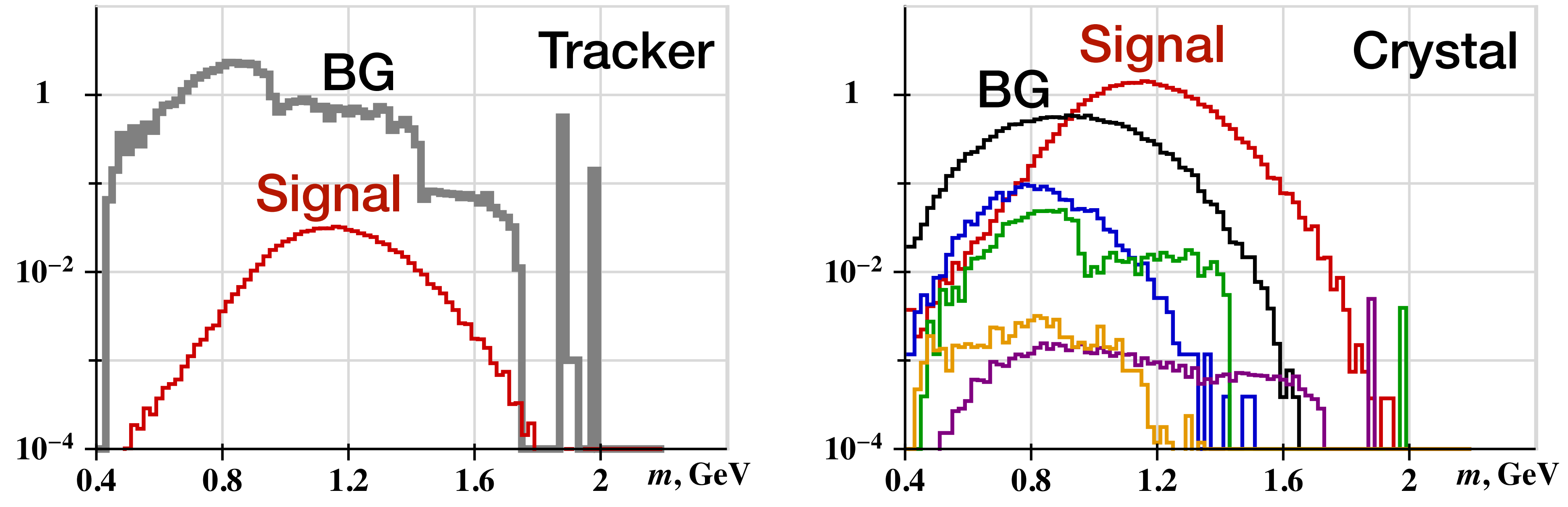

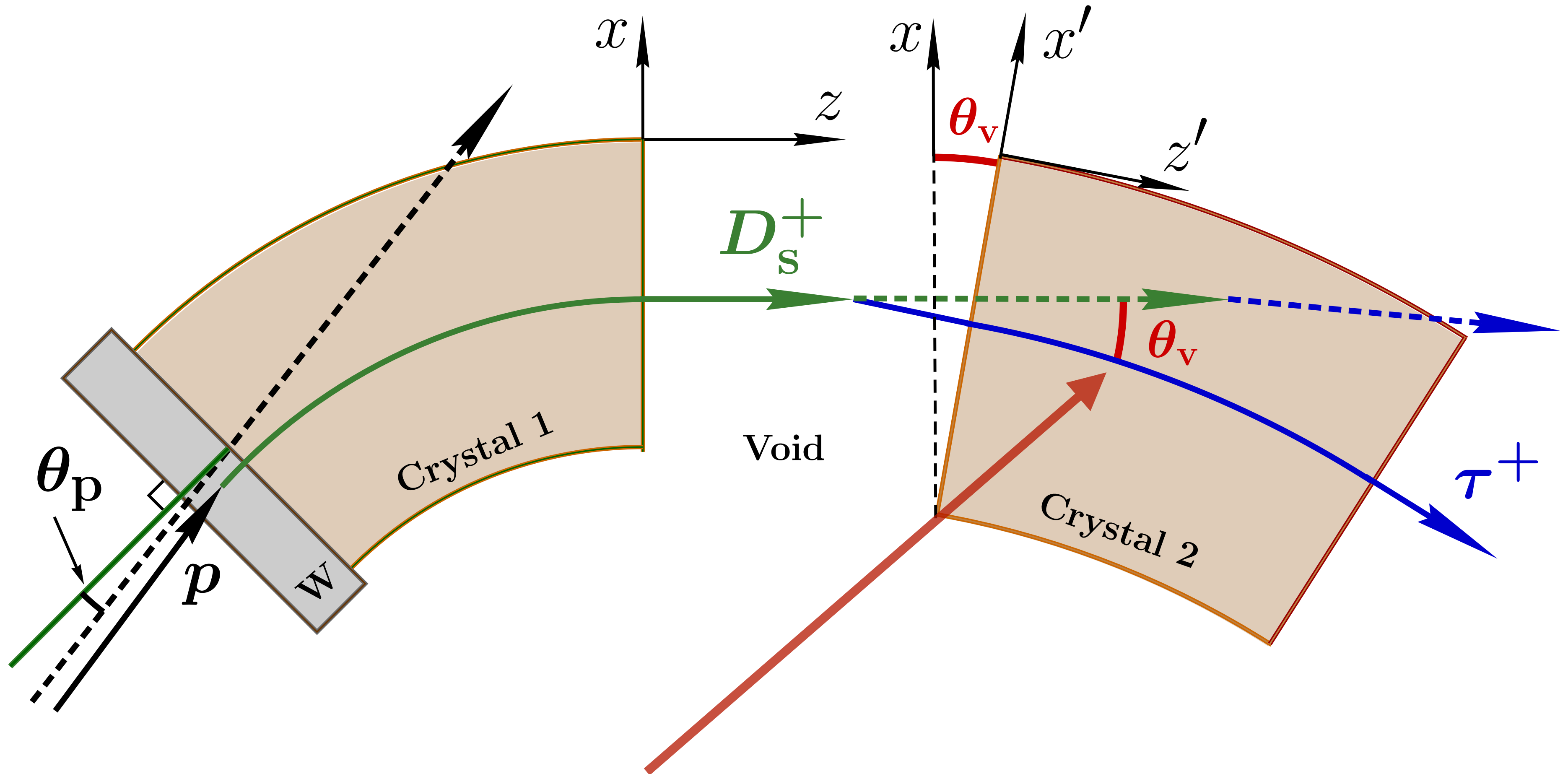

Made a feasibility study of measuring the MDM of Λ_c at the LHC

- Spectra-angular distribution using Pythia + channeling efficiency parametrisation
- optimal layout dimensions
- 10^{16} PoT → current exp. error
- 10^{20} PoT → SM value

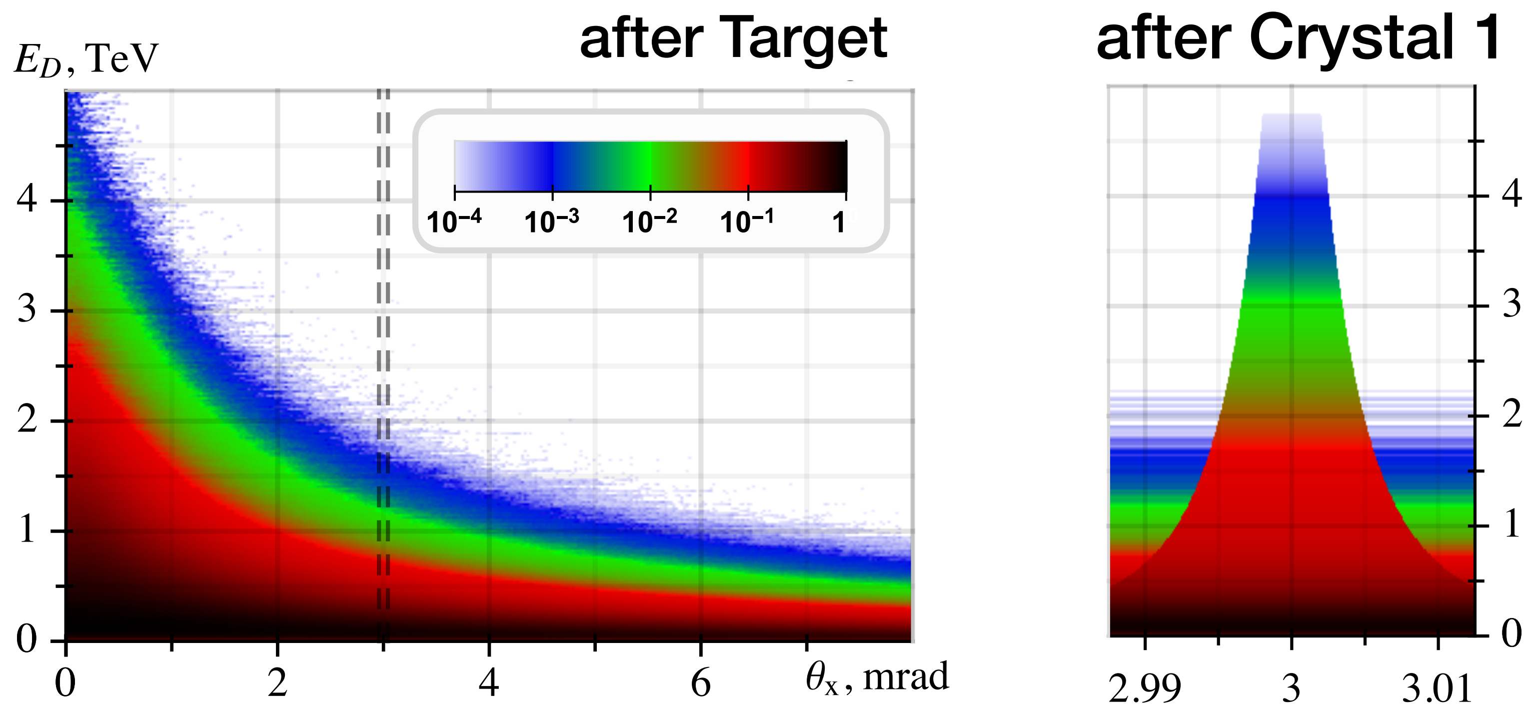

Angular collimation of τ by Crystal 2

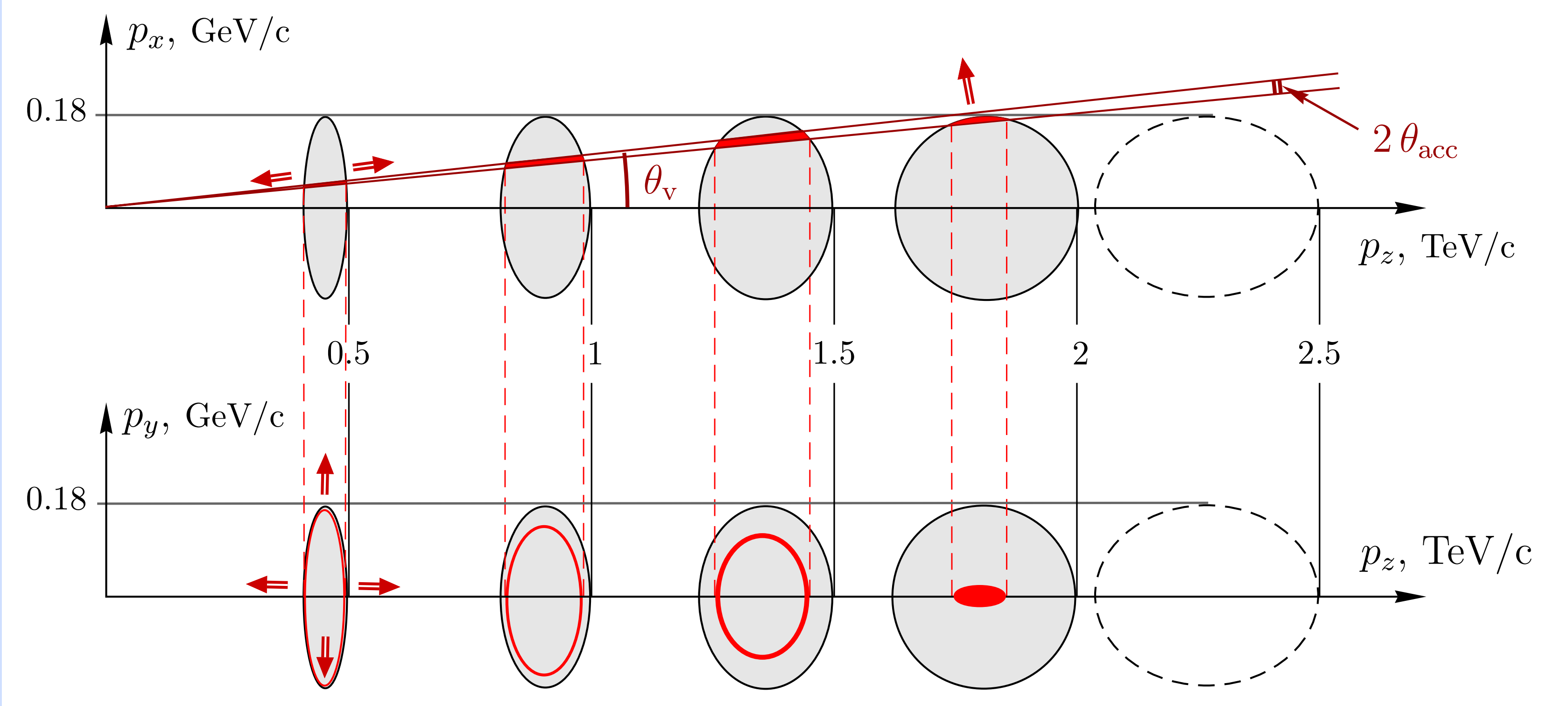

A.S. Fomin et al., JHEP 03 (2019) 156

Thank you

Propagation of the charged particles in crystals *(2015 – 2017)*

Wrote a computer code (Fortran)

- scattering on atoms: binary collision model (on each atom in the row + neighbours)

$$\Delta \vec{\vartheta}_{\mathrm{a}}(\vec{r}) = \frac{Z e^2 \vec{r}}{\varepsilon r^2} \sum_{i=1}^{3} \alpha_i \beta_i^2 K_0(\beta_i r), \quad \Delta \vec{\vartheta}_n = \sum_{k=1}^{N} \Delta \vec{\vartheta}_a(\vec{r}_k)$$

- displacement of nearest atom due to the thermal vibration

$$P(u_x)\, du_x = \frac{1}{\sqrt{2 \pi \overline{u_x^2}}} \exp\left(-\frac{u_x^2}{2 \overline{u_x^2}}\right) du_x$$

- scattering on electrons: aggregate collisions model

$$\vartheta_x^{\mathrm{rms}} = \frac{13.6\ \mathrm{MeV}}{\varepsilon} \sqrt{\frac{\Delta l}{X_0}} \left[1 + 0.038 \ln\left(\frac{\Delta l}{X_0}\right)\right], \quad \frac{\Delta l}{X_0} = \frac{4 e^6}{m^2} \ln(m\, d_{\mathrm{p}}) \int_0^{\Delta l} \bar{n}_e(l)\, dl$$

Found a phenomenological formula for the channeling efficiency as a function of particle energy, crystal bending radius, …

A.Fomin, PhD thesis ⟨NNT : 2017SACLS272⟩

Planar channeling in a bent crystal

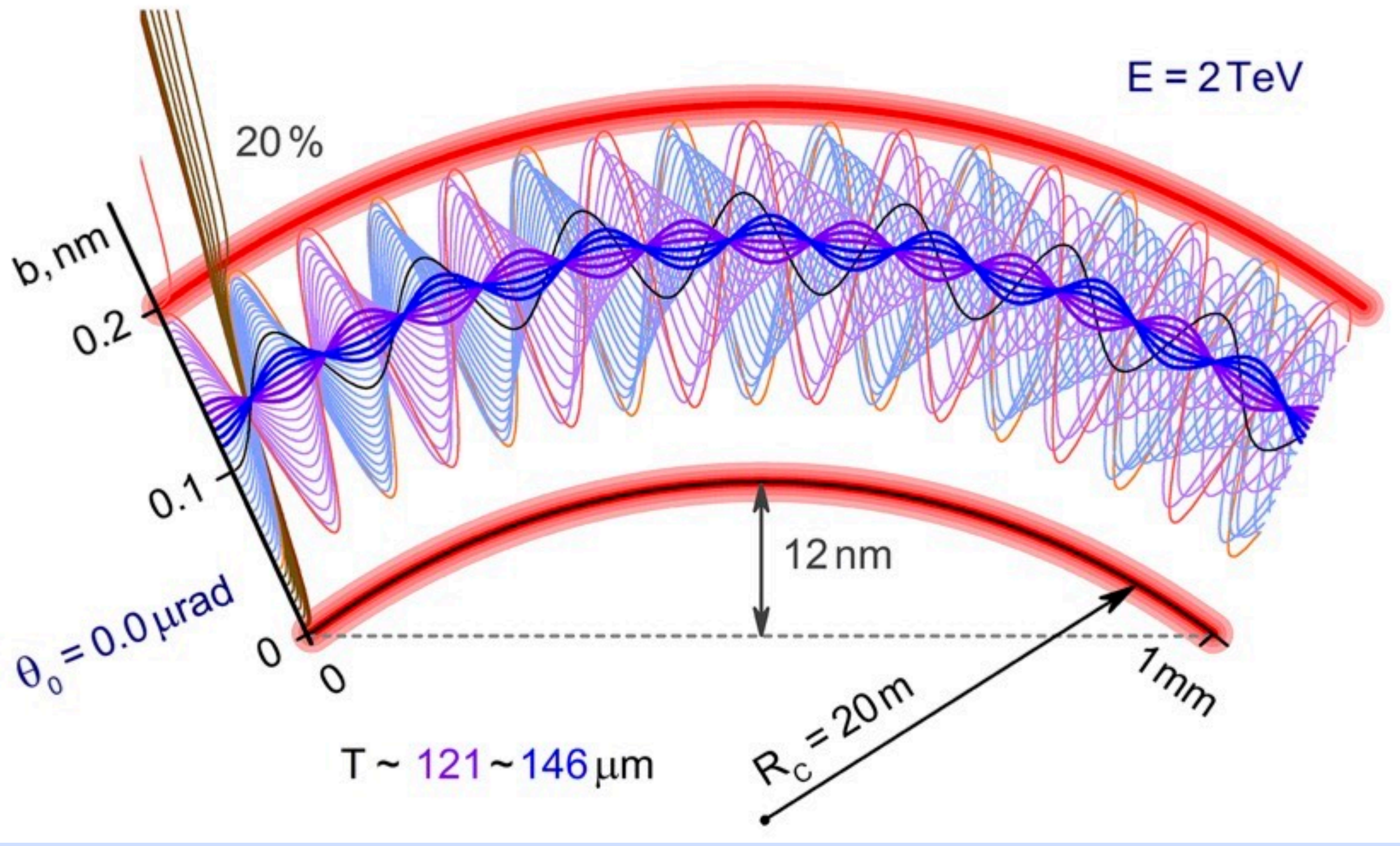

Planar channeling in misaligned bent crystal

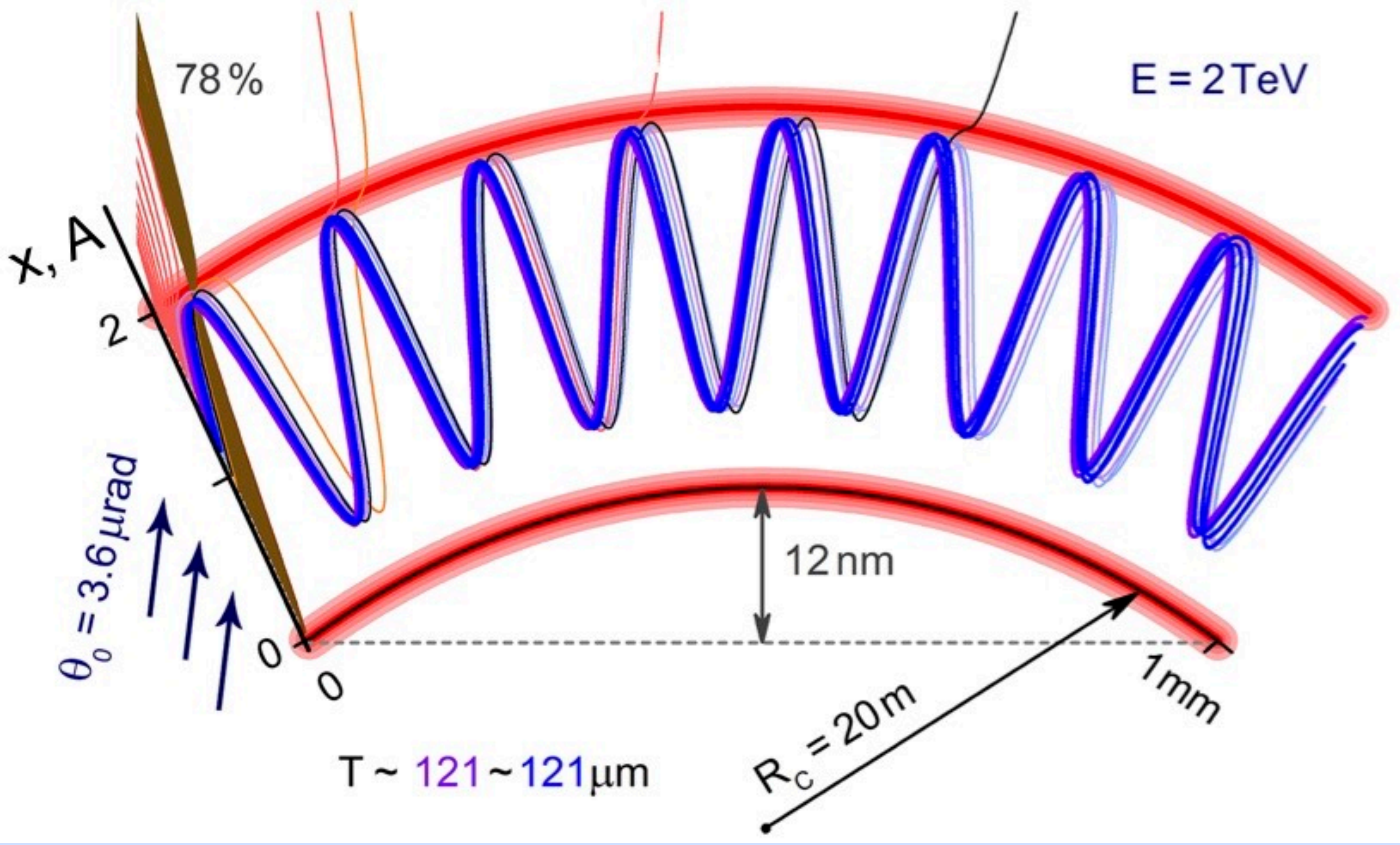

Introduction: initial polarisation in double crystal setup

A. Fomin et al. Eur. Phys. J. C (2020) 80:358 [1909.04654]

Production of Λ_c^+ in a fixed target $p + p \to \Lambda_c^+ + X$

Due to the space-inversion symmetry of the strong interaction

Λ_c^+ polarisation is perpendicular to the reaction plane

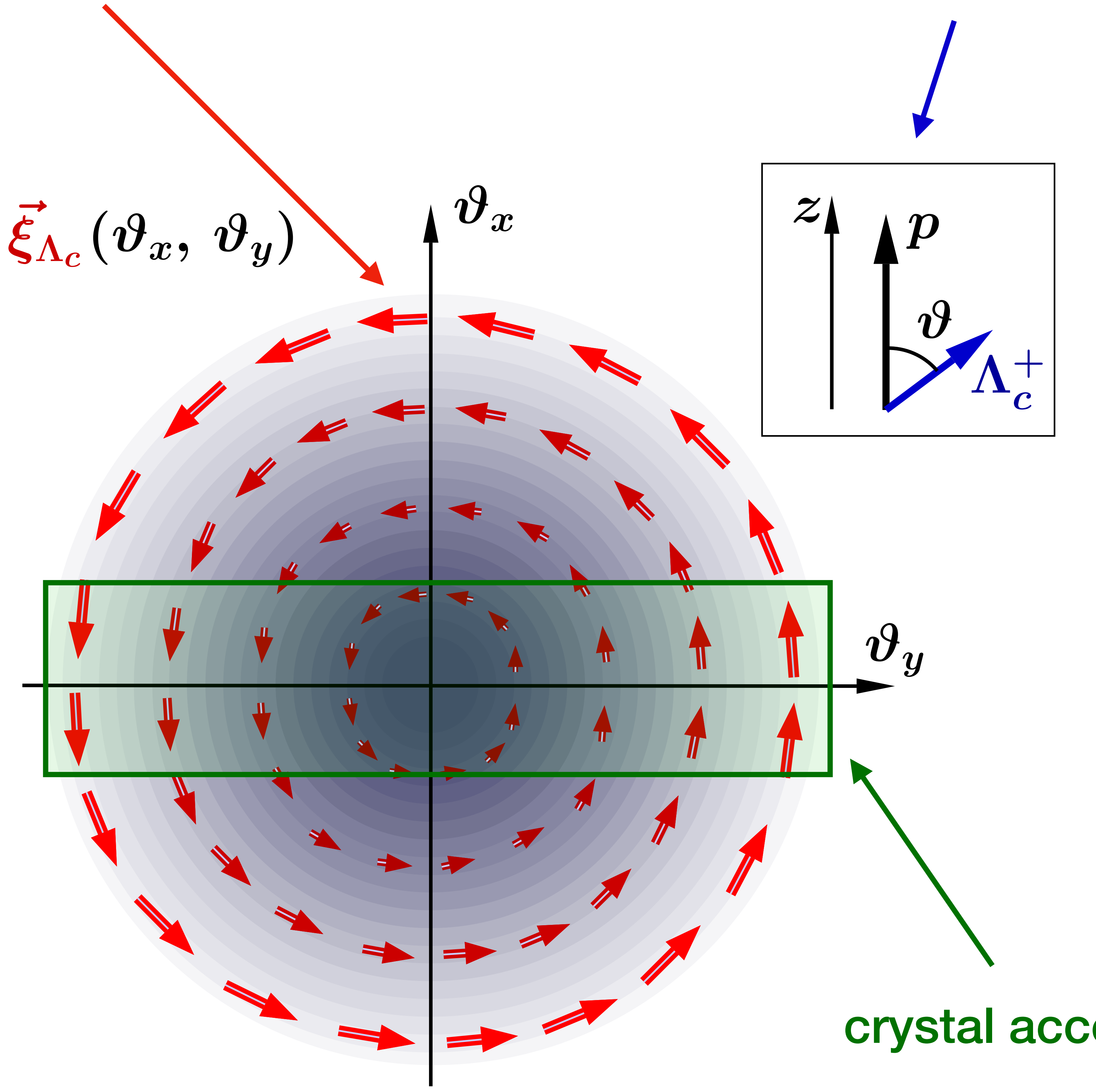

Distribution of Λ_c^+ over transverse momentum (Pythia 8.243)

Initial polarisation as a function of transverse momentum

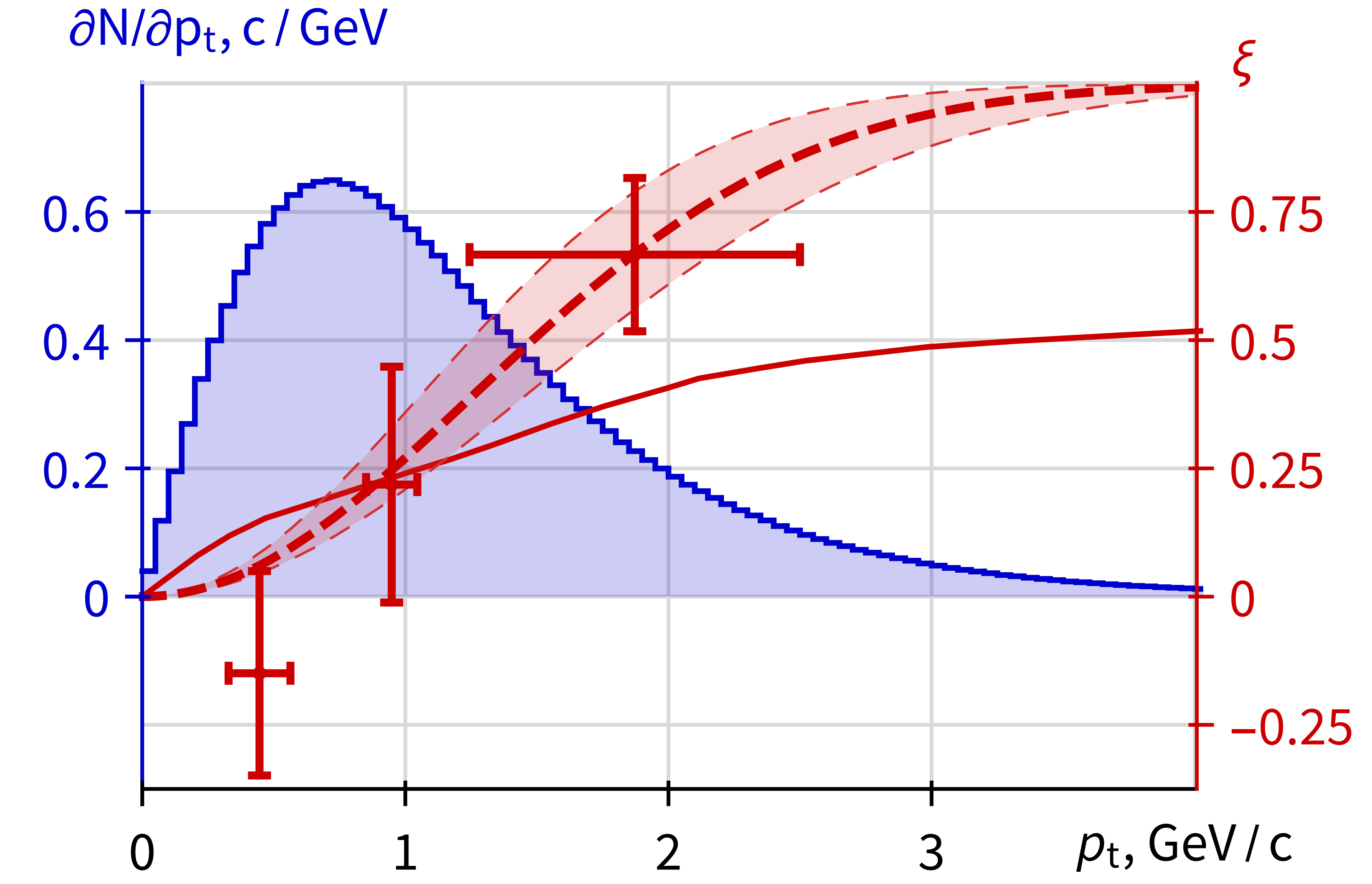

Extrapolated from experimental data $|\xi| = 1 - e^{-\frac{p_t^2}{2\langle p_t^2 \rangle}}$

E791 collaboration, Phys. Lett. B 471 (2000) [inSPIRE]

G.R. Goldstein, hep-ph/0001187 (2000) [inSPIRE]

MDM of Σ^+ experiment E761, Fermilab 1990: Mirror the setup — double the statistics

D. Chen, The Measurement of the Magnetic Moment of Σ+ Using Channeling in Bent Crystals, PhD thesis, SUNY, Albany, 1992.

crystal #5

crystal #2

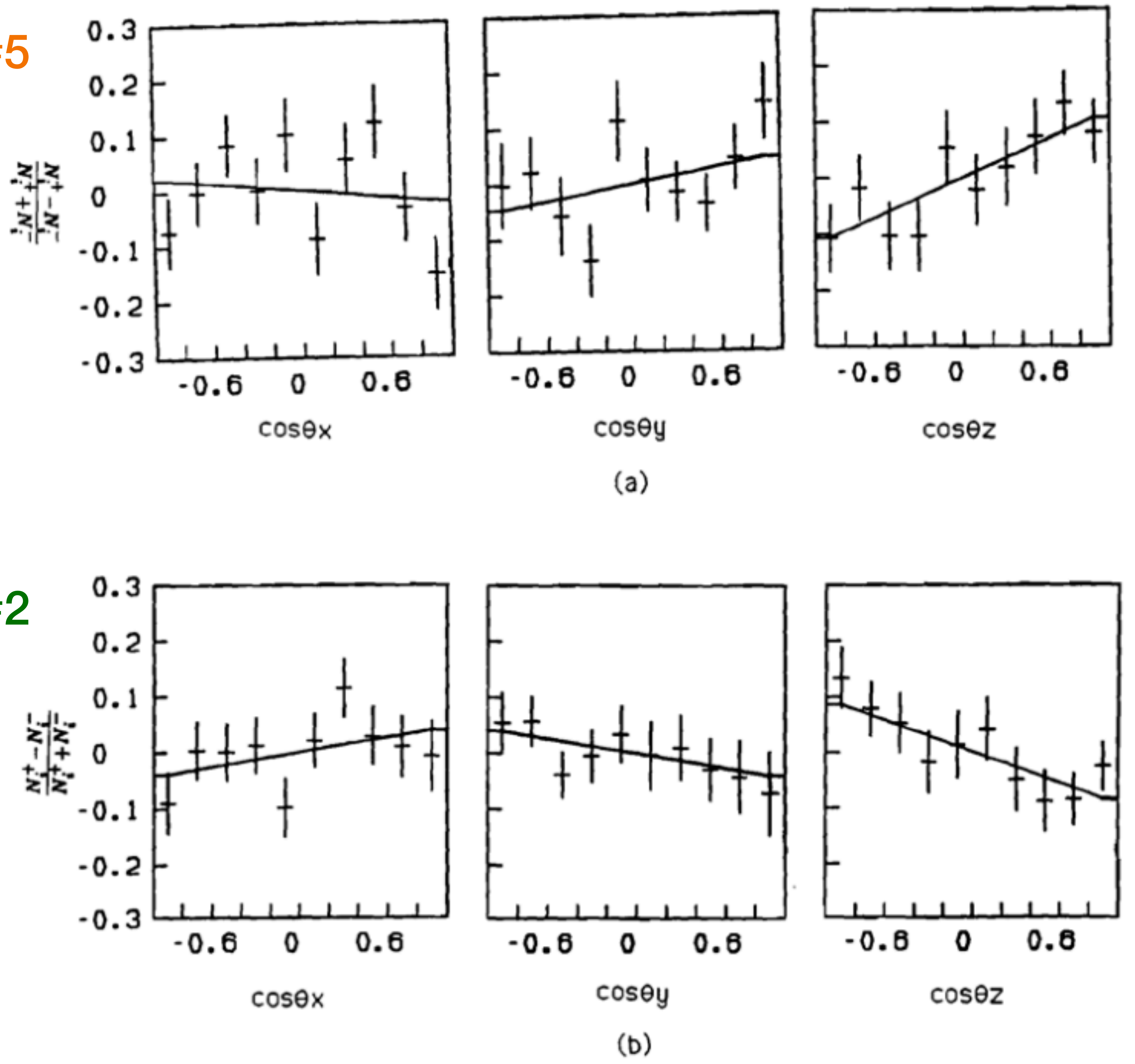

Figure 8.5: The $\frac{N_i^+ - N_i^-}{N_i^+ + N_i^-}$ distribution of the events in the signal area for (a) the 5th crystal and (b) the 2nd crystal.

Separate analyses have been done for crystal #5 and #2

We used a bias cancelling technique to cancel the A_i. The distribution of the data with a positive targeting angle, i.e. with the polarization $\mathbf{P}^+$, can be written as

$$\frac{dN_i^+}{N_{0i}^+ d\cos\theta_i} = \frac{1}{2}A_i(1 + \alpha \mathbf{P}_i^+ \cos\theta_i). \tag{8.3}$$

And the equation for negative targeting angle, i.e. with the polarization $\mathbf{P}^-$, is

$$\frac{dN_i^-}{N_{0i}^- d\cos\theta_i} = \frac{1}{2}A_i(1 + \alpha \mathbf{P}_i^- \cos\theta_i). \tag{8.4}$$

Assuming the same amplitude for the positive and the negative targeting angle, $\mathbf{P}_i^+ = -\mathbf{P}_i^-$, we can rewrite equation (8.4) as

$$\frac{dN_i^-}{N_{0i}^- d\cos\theta_i} = \frac{1}{2}A_i(1 - \alpha \mathbf{P}_i^+ \cos\theta_i). \tag{8.5}$$

If we redefine $N_i^+ = \frac{dN_i^+}{N_{0i}^+ d\cos\theta_i}$ and $N_i^- = \frac{dN_i^-}{N_{0i}^- d\cos\theta_i}$ and assume that A_i is the same for both targeting angles, from equation (8.3) and equation (8.5), we can derive

$$\frac{N_i^+ - N_i^-}{N_i^+ + N_i^-} = \alpha \mathbf{P}_i^+ \cos\theta_i. \tag{8.6}$$

From the plot of $\frac{N_i^+ - N_i^-}{N_i^+ + N_i^-}$ versus $\cos\theta_i$, we obtained the $\alpha\mathbf{P}_i^+$ from the slope of the distribution.

	$\mu_{\Sigma+}$ (μ_N) with channeling cut	$\mu_{\Sigma+}$ (μ_N) no channeling cut
5th crystal	2.15 ± 0.61	2.32 ± 0.58
2nd crystal	2.74 ± 0.71	2.62 ± 0.73
Average	2.40 ± 0.46	2.44 ± 0.46
PGD	2.42 ± 0.05	

Table 8.4: Results of the $\mu_{\Sigma+}$ measurement with statistical error only.

Systematical error of g-factor from poor knowledge of α and ξ

A. Fomin et al. Eur. Phys. J. C (2020) 80:358

1) use pre-measured values of $\alpha\cdot\xi$ factor

2) measure $\alpha\cdot\xi$ and g-factor simultaneously

$$\frac{dN}{d\cos\theta_z} = \frac{1}{2}\left(1 + \alpha\,\xi_z\,\cos\Theta_\mu\,\cos\theta_z\right)$$

$$\frac{dN}{d\cos\theta_x} = \frac{1}{2}\left(1 + \alpha\,\xi_x\,\sin\Theta_\mu\,\cos\theta_x\right)$$

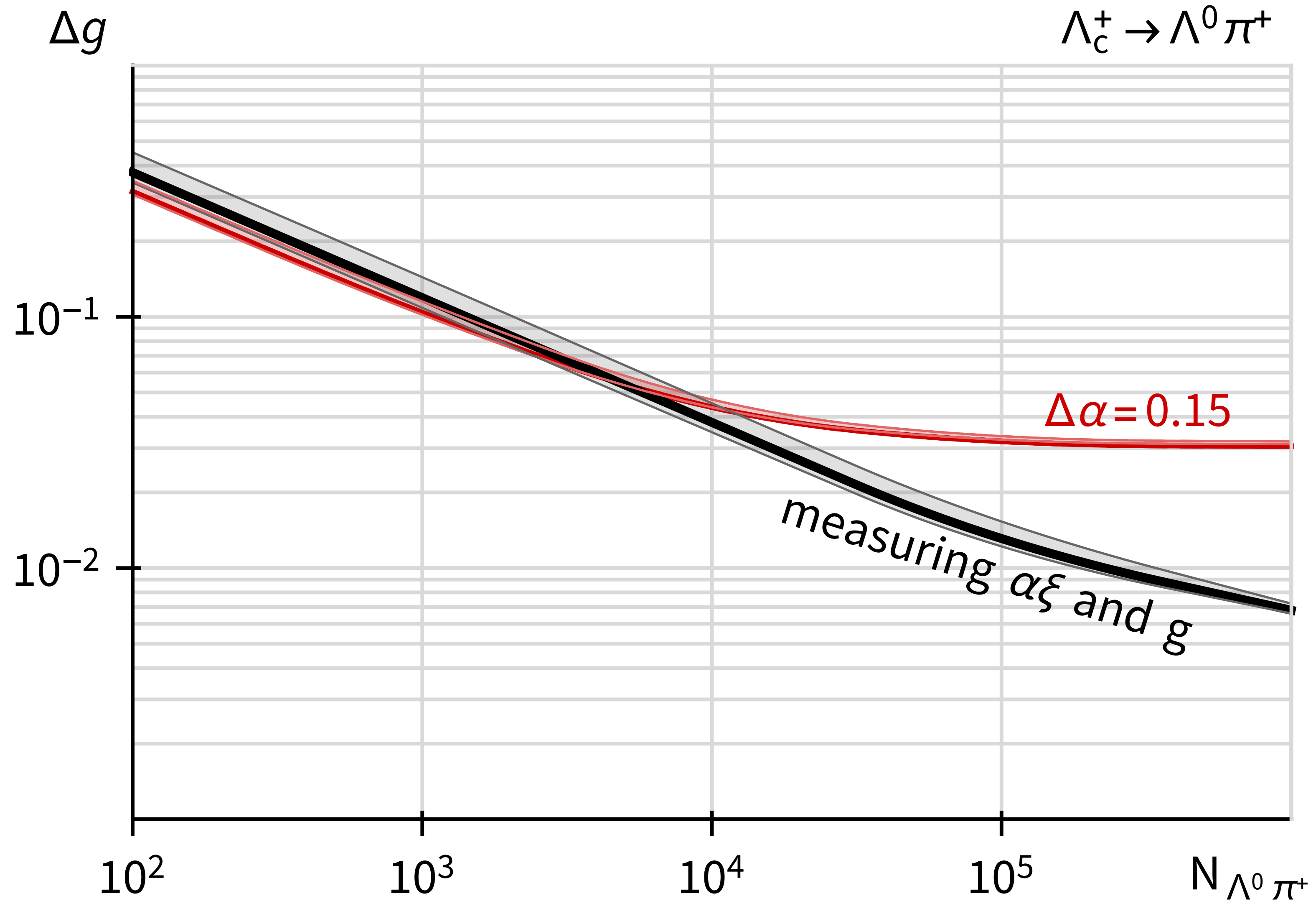

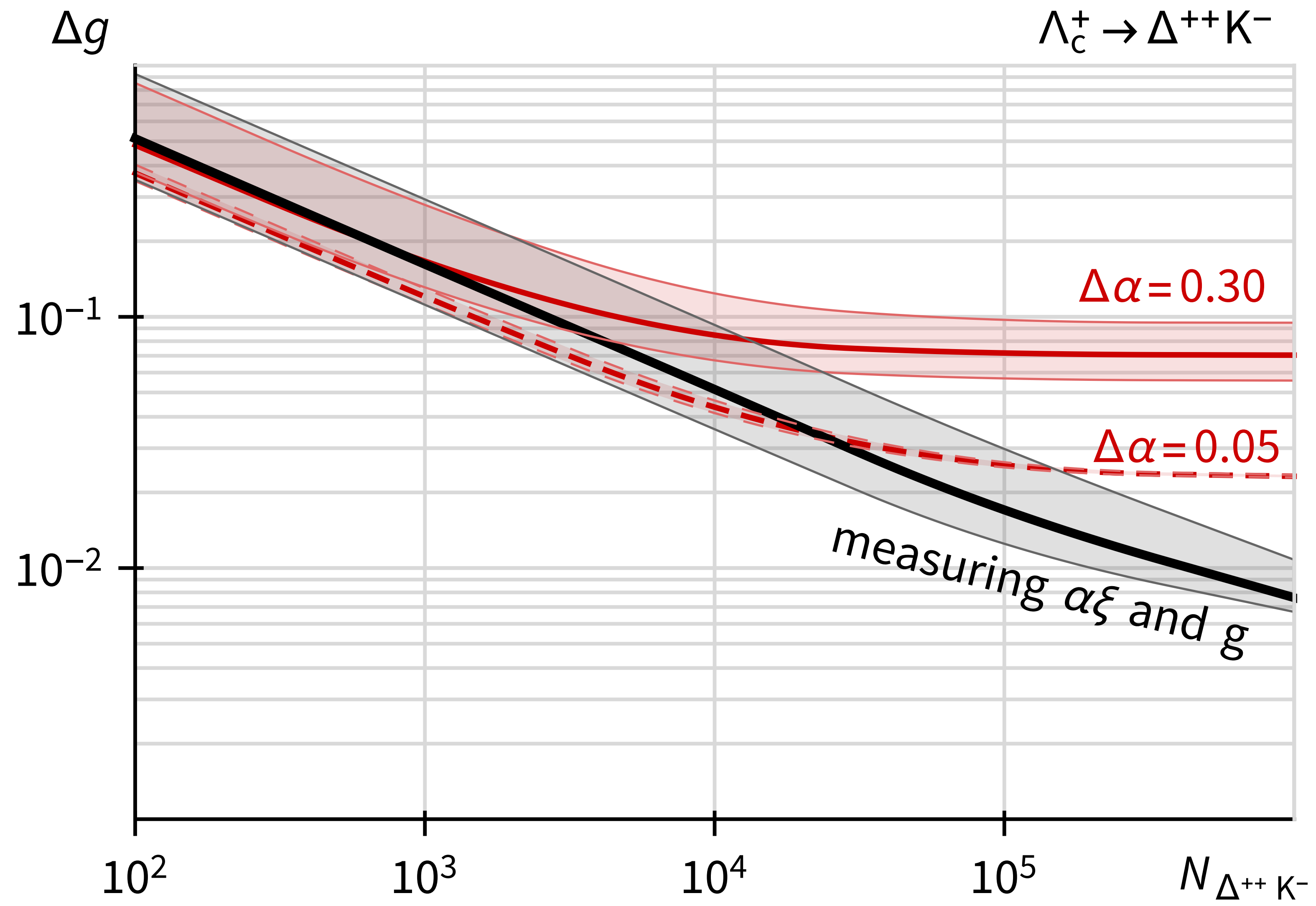

Decay channel	Branching ratio, %	Weak decay parameter α	Detector efficiency		Wieght $(\Delta g/\Delta gj)^2$
			IR3	IR8*	
$\Lambda_c^+ \to p\,K^*(892)$	1.96(27)	0.66(28)	0.2	0.2	~ **0.60**
$\Lambda_c^+ \to \Delta^{++}(1232)\,K^-$	1.08(25)	−0.67(**30**)	0.2	0.2	~ **0.35**
$\Lambda_c^+ \to \Lambda(p\pi^-)\,\pi^+$	0.83(5)	0.91(**15**)	0.02	0.004	0.01–0.05
$\Lambda_c^+ \to \Lambda(1520)\,\pi^+$	2.20(5)	−0.11(60)	0.2	0.2	0.02

* E. Bagli et al., EPJ C77 (2017) no.12, 828

Channeling in a long crystal

Acceptance angle

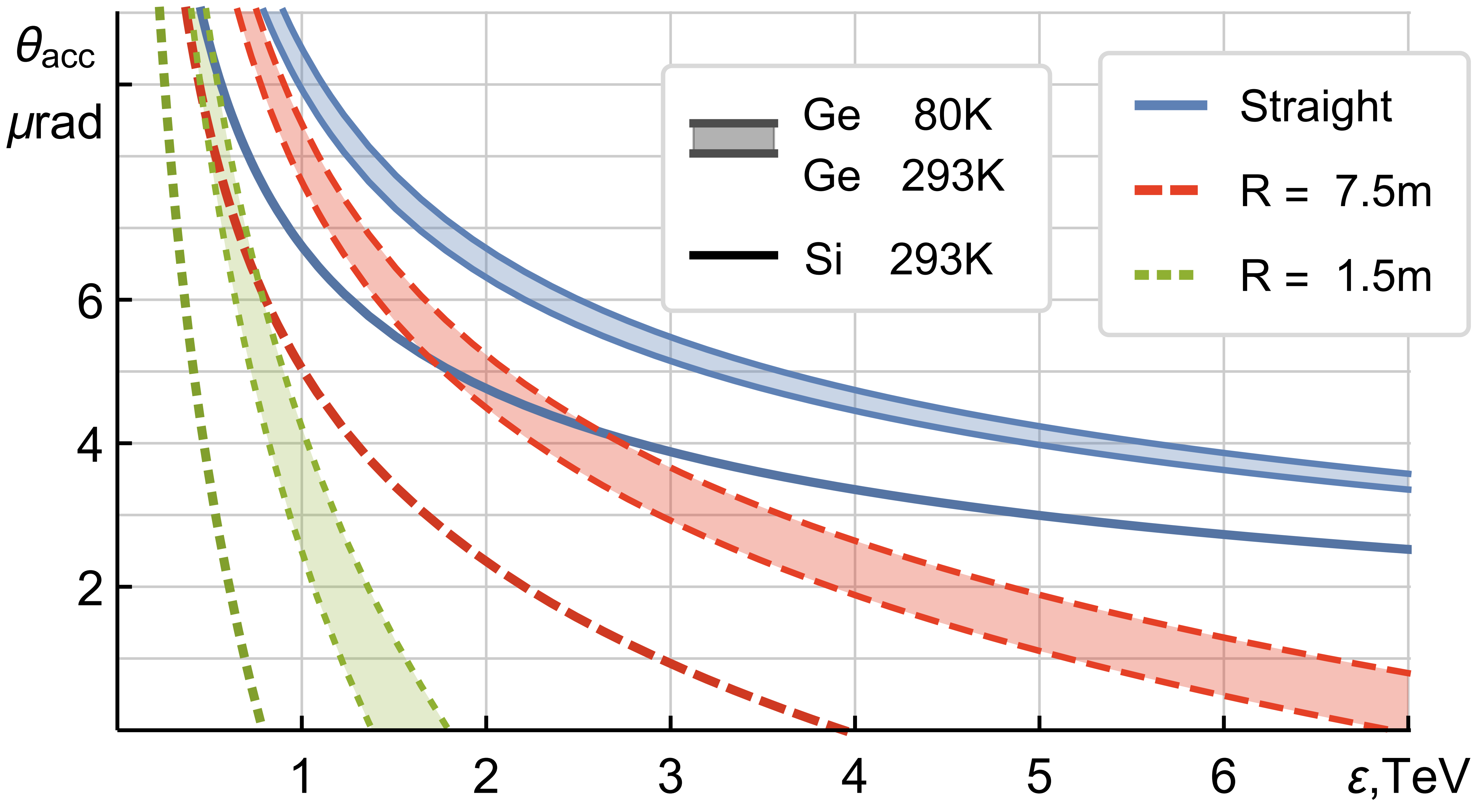

$$\theta_{\mathrm{acc}} = \sqrt{\frac{2\,U_{\mathrm{eff}}}{\varepsilon}\left(1 - \frac{\varepsilon}{R}\frac{1}{U'_x}\right)}$$

Crystal	T, °K	U_{eff}, eV	U'_x, TeV/m
Si	293	22.8	0.525
Ge	293	40.0	0.922
Ge	80	45.2	1.200

Channeling in a bent crystal: acceptance factor

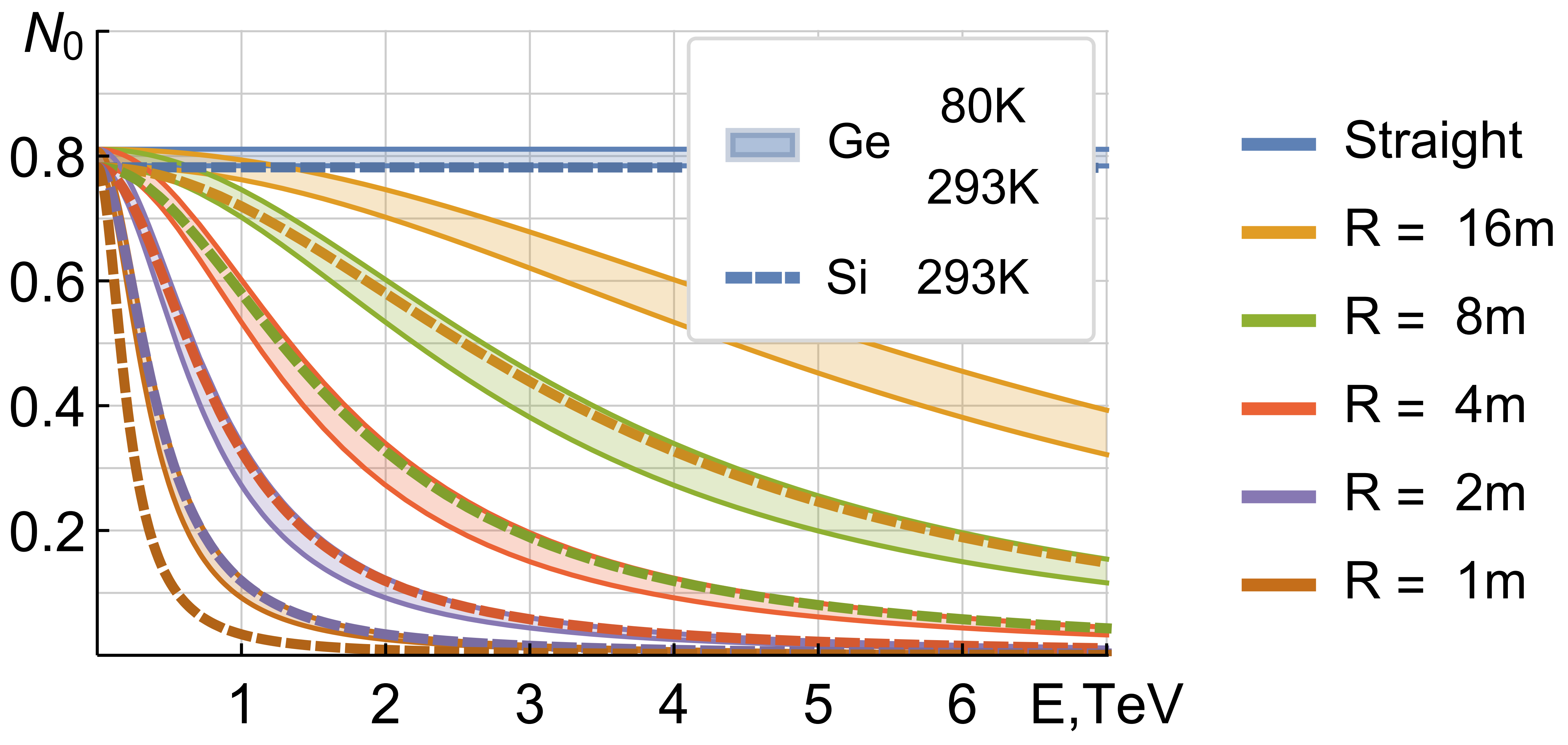

$$\eta_{\text{ch}}\left(\varepsilon, R\right) = \frac{\eta_{\text{str}}}{1 + \left(\dfrac{\varepsilon}{R} \; \dfrac{1}{U_x' \, k_\theta}\right)^2}$$

Crystal	T, $^\circ$K	U_x', TeV/m	η_{str}	k_θ
Si	293	0.525	0.775	0.405
Ge	293	0.922	0.785	0.396
Ge	80	1.200	0.812	0.353

Channeling in a bent crystal: dechanneling length

Dechanneling probability

$$\eta_{\mathrm{dech}}(\varepsilon, R, L) = 1 - \mathrm{e}^{-\sqrt{\frac{L}{L_{\mathrm{dech}}(\varepsilon, R)}}}$$

Dechanneling length

$$L_{\mathrm{dech}}(\varepsilon, R) = L_{\max} \frac{\varepsilon}{\varepsilon_{\max}} \; \mathrm{e}^{1 - \frac{\varepsilon}{\varepsilon_{\max}}}$$

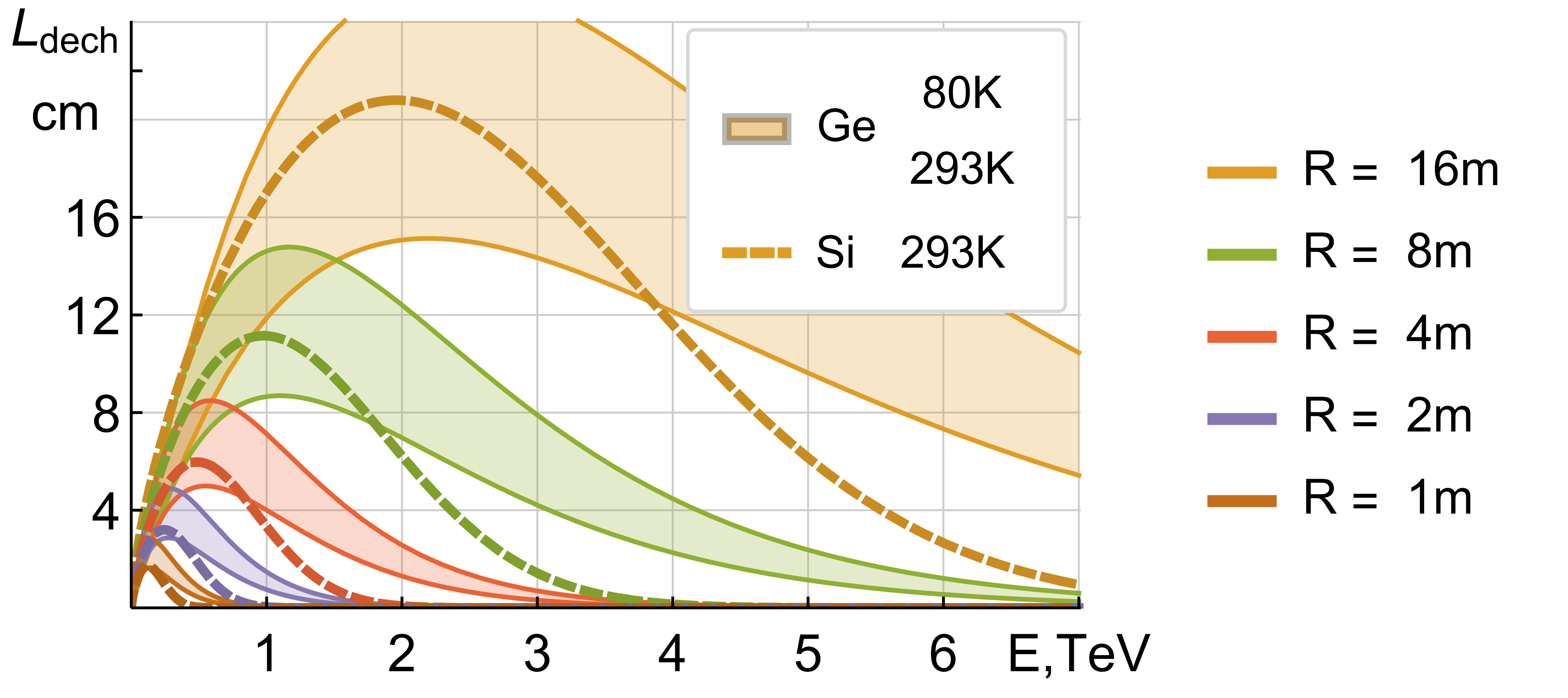

$$L_{\max} = k_{\mathrm{dech}} R \left(\frac{R_0}{R}\right)^{b_{\mathrm{dech}}}$$

$$\varepsilon_{\max} = R \; F_{\mathrm{dech}}$$

Crystal	$T, ^{\circ}$K	k_{dech}	R_0, m	b_{dech}	F_{dech}, TeV/m
Si	293	0.0146	3.7	0.1	0.097
Ge	293	0.0130	3.3	0.2	0.137
Ge	80	0.0226	2.9	0.2	0.146

Active bunch excitation

Bunch excitation: Profile of collimated bunch

Due to betatron oscillation all the particles with emittance $\varepsilon > \varepsilon_{coll}$ hit the collimation system → Assuming the linear machine this leads to a cut in the emittance distribution at $\varepsilon = \varepsilon_{coll}$ → cut of the bunch profile at $\sigma_b > \sigma_{coll}$ and reduction of bunch core population

$$\begin{cases} \sqrt{\beta\varepsilon_0} = \sigma_0 \\ \sqrt{\beta\varepsilon_{coll}} = y_{coll} = 5\,\sigma_0 \end{cases} \rightarrow \quad \frac{\varepsilon_{coll}}{\varepsilon_0} = 25$$

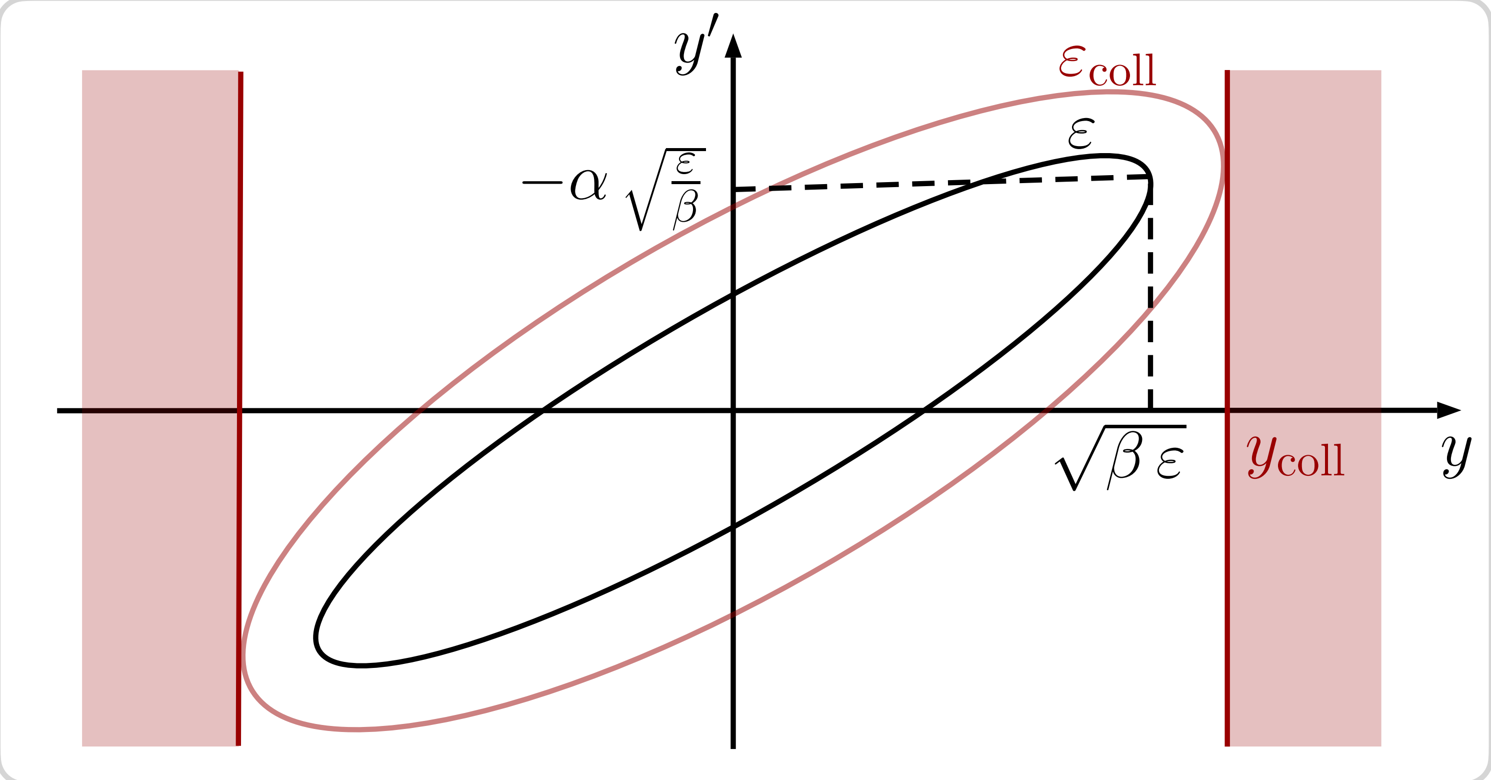

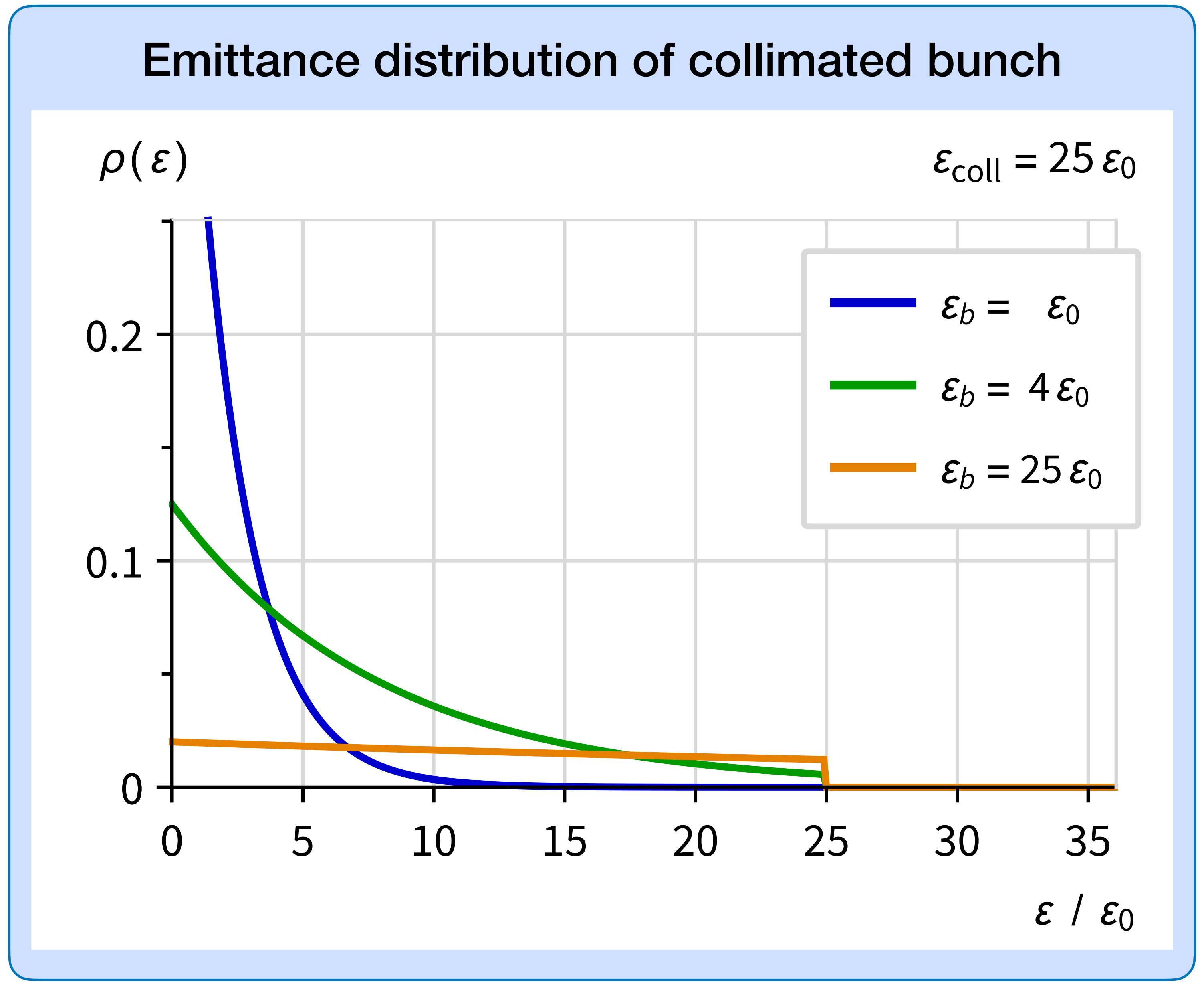

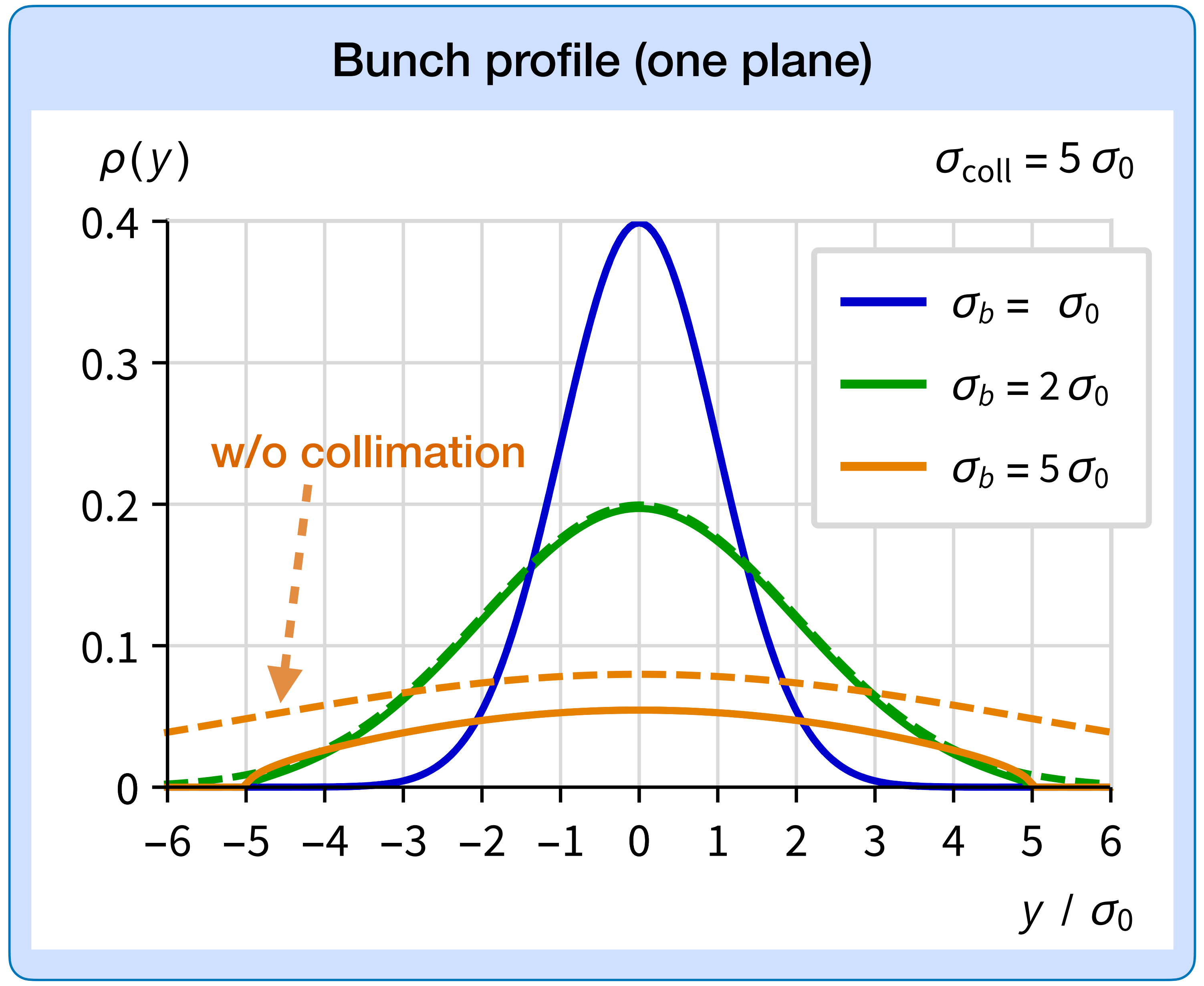

$$\begin{cases} \rho(\varepsilon, \varepsilon_b) = \dfrac{1}{2\,\varepsilon_b}\exp\left(-\dfrac{\varepsilon}{2\,\varepsilon_b}\right) & \varepsilon < \varepsilon_{coll} \\ \rho(\varepsilon, \varepsilon_b) = 0 & \varepsilon > \varepsilon_{coll} \end{cases}$$

$$\rho(y, \sigma_b) = \frac{1}{\sqrt{2\pi}\sigma_b}\ \exp(-\frac{y^2}{2\,\sigma_b^2})\ \mathrm{Erf}\sqrt{\frac{\frac{\varepsilon_{coll}}{\varepsilon_0} - \frac{y^2}{\sigma_0^2}}{2\,\sigma_b^2/\sigma_0^2}}$$

where ε_b and σ_b are the emittance and the size of the bunch without collimation

Bunch excitation: Luminosity reduction

Profile of collimated bunch, that w/o collimation (gaussian shape) would have rms width σ_b

$$\rho(y,\sigma_b) = \frac{1}{\sqrt{2\pi}\sigma_b}\ \exp(-\frac{y^2}{2\,\sigma_b^2})\ \mathrm{Erf}\sqrt{\frac{\frac{\varepsilon_{coll}}{\varepsilon_0} - \frac{y^2}{\sigma_0^2}}{2\,\sigma_b^2/\sigma_0^2}}$$

Relative luminosity: the decrease of the current luminosity due to beam 1 excitation in y-direction

$$\eta_L^{cur}(t) = \frac{L'_{cur}(t)}{L_{cur}(t)} = \frac{n'_1(t)}{n_1(t)}\ \frac{\int \rho'_{y1}\,\rho_{y2}\,dy}{\int \rho_{y1}\,\rho_{y2}\,dy}$$

Separating the time and from-factor dependent parts of this factor

$$\eta_L^{tot}(t) = \eta_t^{tot}(t)\ \eta_\rho$$

The from-factor dependent part of relative luminosity

Collimation

$$\eta_\rho = \frac{\int \rho'_{y1}\,\rho_{y2}\,dy}{\int \rho_{y1}\,\rho_{y2}\,dy} = \frac{2\sqrt{\pi}}{2\pi\,\sigma_b\,\sigma_0}\int_{-\sigma_{coll}}^{\sigma_{coll}} dy\ \exp\left(-\frac{y^2}{2\sigma_0} - \frac{y^2}{2\sigma_b}\right) \mathrm{Erf}\sqrt{\frac{\sigma_{coll}^2 - y^2}{2\sigma_b^2}}$$

Bunch profile (one plane)

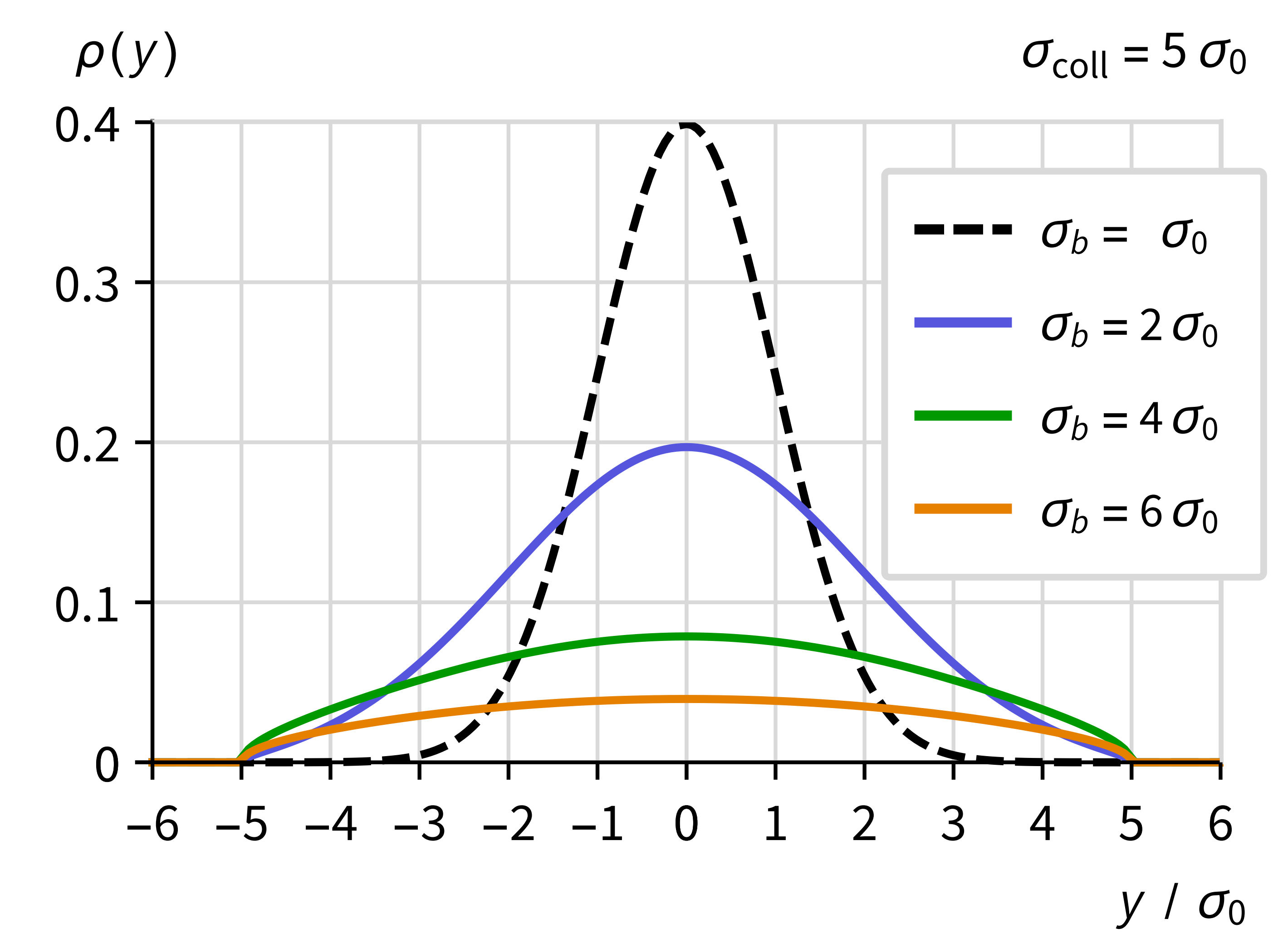

Relative luminosity and Collimation losses

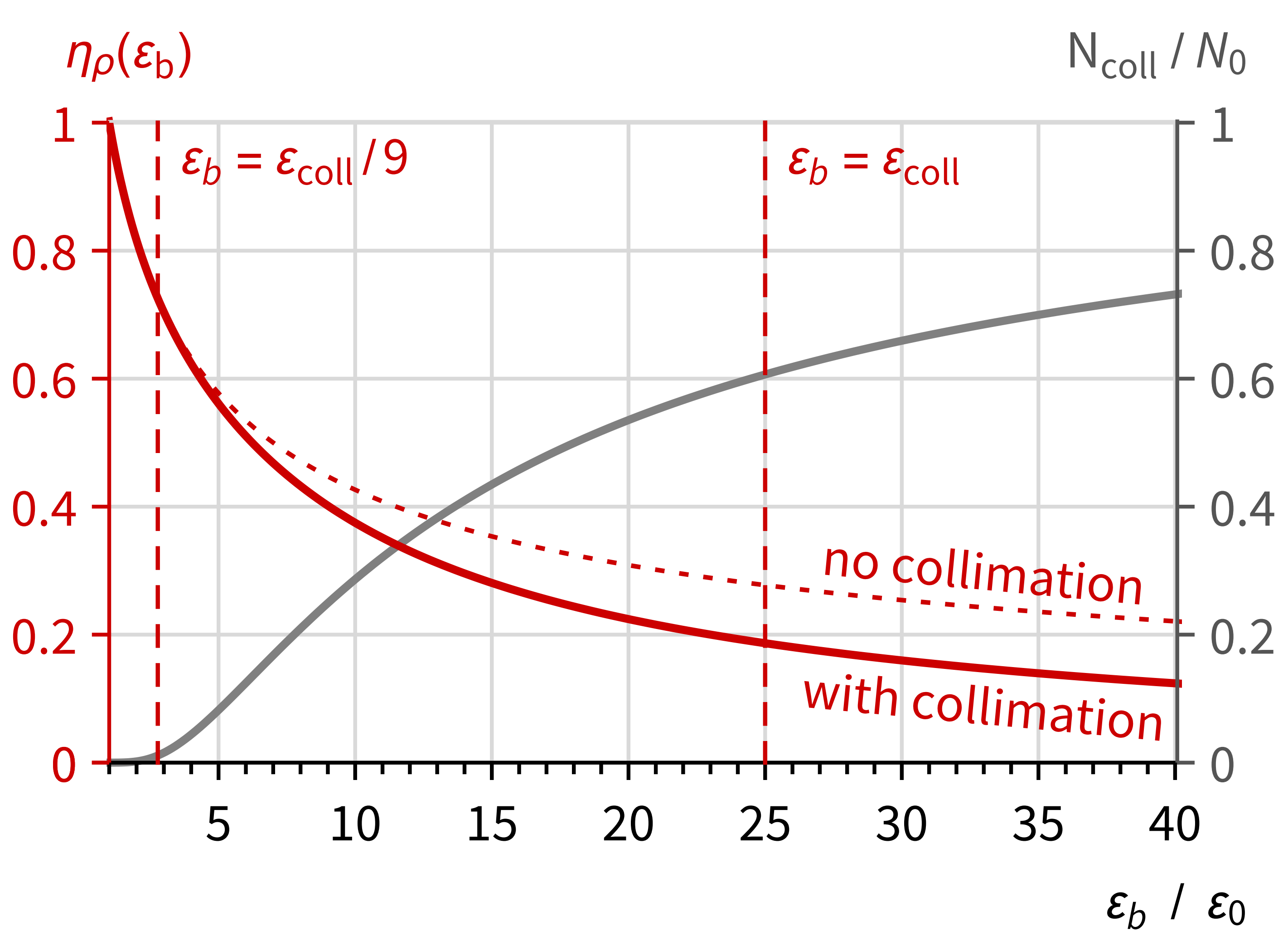

Maximum achievable PoT due to beam excitation (based on 2018 run data)

The gain factor in PoT from the beam excitation with respect to the “Baseline” (no excitation):

$$\eta_{exc} = \frac{N_{PoT}^{(ex)}}{N_{PoT}^{(BL)}}$$

too high rates of PoT per bunch crossing (~49 @LHCb)

					200 kW in coll. system		3.5 p / bunch X @ LHCb		
					after collisions			after collis.	during collis.
Beam excitation	N_{coll}	N_{PoT} (IR3)	N_{PoT} (IR8)	η_{exc}	*t, h*	*ΔL / L*	t, h	ΔL / L	ΔL / L
No excitation (“Baseline”)	1.7×10^{15}	4.7×10^{12}	6.8×10^{12}	1	*1908*	*0*	1908	0	0
All fills, no limit on Δt	4.7×10^{15}	2.6×10^{13}	3.8×10^{13}	5.6	*8*	*> 0.4 %*	167	8.7 %	2.9 %
Selected fills (2556b), Δt < 1 hour	2.5×10^{15}	1.4×10^{13}	2.0×10^{13}	3.0	-	-	54	2.8 %	1.2 %

The most efficient scenario:

The gradual excitation of bunches (3.5 p/bunch X) at the end of the fills with 2556 bunches, with duration under 1 hour:

⇒ delivers **3 times more PoT** w.r.t. “Baseline”

⇒ reduces the total luminosity at ATLAS and CMS by **~1.2%**